

Conserved Quantities from Entanglement Hamiltonian

Biao Lian¹

¹*Department of Physics, Princeton University, Princeton, New Jersey 08544, USA*

(Dated: April 29, 2022)

We show that the subregion entanglement Hamiltonians of typical excited eigenstates of a quantum many-body system are approximately linear combinations of local or quasilocal conserved quantities of the subregion. By diagonalizing an entanglement Hamiltonian superdensity matrix (EHSM) for an ensemble of eigenstates, we can obtain the subregion (quasi)local conserved quantities as the EHSM eigen-operators with nonzero eigenvalues. For free fermions, we find the number of nonzero EHSM eigenvalues is around the order of subregion volume. In the interacting XYZ model (within sizes calculable), we find the nonzero EHSM eigenvalues decay roughly in power law if the system is integrable, with the exponent $s \approx 1$ if the eigenstates are extended, and $s \approx 1.5 \sim 2$ if the eigenstates are many-body localized. For fully chaotic systems, only two EHSM eigenvalues are significantly nonzero, the eigen-operators of which correspond to the identity and the subregion Hamiltonian.

Conserved quantities significantly affect the integrability and non-equilibrium dynamics of a quantum many-body system, for instance, they may lead the system to equilibrate into a non-thermal state described by a generalized Gibbs ensemble [1–5]. In quantum systems, the generic belief is that only local and quasilocal conserved quantities contribute to the quantum integrability. However, unlike classical systems, it is not clear how many (quasi)local conserved quantities are generically needed for a quantum system to be integrable. Moreover, it is difficult to find all the local and quasilocal conserved quantities even for exactly solvable models [6–9], and it is unclear whether all of them contribute to the quantum integrability.

Two frequently employed indicators distinguishing between chaotic and integrable systems are the level spacing statistics (LSS) [10, 11] and the eigenstate thermalization hypothesis (ETH) [12–16]. However, neither LSS nor ETH can give much information (e.g., conserved quantities) about a quantum system which is not fully chaotic. The other feature of quantum chaos is the Lyapunov exponent in the out-of-time-ordered correlation [17]. This, however, usually requires certain large flavor limit, for instance in the Sachdev-Ye-Kitaev type models [18–22].

Here we ask, given the many-body eigenstates of a quantum system, can one obtain the (quasi)local conserved quantities and tell the integrability of the system? Previous studies show that a strictly local Hamiltonian can be recovered from a single eigenstate [23]. For chaotic systems, ETH suggests that the subregion entanglement Hamiltonian resembles the physical Hamiltonian [24]. In this letter, we show that the entanglement Hamiltonians of typical excited eigenstates of a quantum system in a subregion are approximate linear combinations of the (quasi)local conserved quantities in the subregion. Given the entanglement Hamiltonians of an ensemble of eigenstates, one can define an entanglement Hamiltonian superdensity matrix (EHSM), the eigen-operators of which with nonzero eigenvalues resemble the subregion conserved quantities. For free fermions [25], we find the number of nonzero EHSM eigenvalues is around the order of the subregion volume. We further investigate

the interacting 1D XYZ model with (without) disorders (within sizes calculable), where we find the n -th largest EHSM eigenvalue decays as n^{-s} if the system is integrable. The exponent $s \approx 1$ if the system is delocalized, and $s \approx 1.5 \sim 2$ if the system shows many-body localization (which is arguably integrable) [26–34]. For fully chaotic systems where the ETH holds, only two EHSM eigenvalues are significantly nonzero, corresponding to the only two (quasi)local subregion conserved quantities: the identity and the physical Hamiltonian. We conjecture that the conserved quantities in the EHSM are those governing the quantum integrability.

— *Entanglement Hamiltonian.* We shall consider quantum systems in lattices, and assume each lattice site has a finite Hilbert space dimension d . Consider a system in a finite real space region with L sites, which has a Hilbert space dimension $N = d^L$. Assume the system has a local $N \times N$ many-body Hamiltonian H in this region, and has eigenstates $|\alpha\rangle$:

$$H|\alpha\rangle = E_\alpha|\alpha\rangle, \quad (1)$$

where E_α is the energy of eigenstate $|\alpha\rangle$ ($1 \leq \alpha \leq N$). We divide this region into two subregions A and B with number of sites L_A and $L_B = L - L_A$ (Fig. 1), which have Hilbert space dimensions $N_A = d^{L_A}$ and $N_B = d^{L_B}$, respectively. We denote the boundary number of sites between A and B as l_{AB} . The Hamiltonian H can then be divided into

$$H = H_A \otimes I_B + I_A \otimes H_B + H_{AB}, \quad (2)$$

where I_A and I_B are the identity matrix in A and B subregions, $H_A \otimes I_B$ ($I_A \otimes H_B$) contains all the product terms with supports within subregion A (B) (including the identity term $I_A \otimes I_B$), while H_{AB} denotes all the product terms with supports across subregions A and B . Here a product term is defined as the product $\prod_{j \in \mathcal{S}} \mathcal{O}_j$ of traceless on-site operators \mathcal{O}_j of a set of sites \mathcal{S} , and the set of sites \mathcal{S} is called the *support*. Note that $\text{tr}(H_{AB}) = 0$. Therefore, H_A and H_B can be understood as the bulk Hamiltonian of subregions A and B , while H_{AB} is the boundary coupling between subregions A and B .

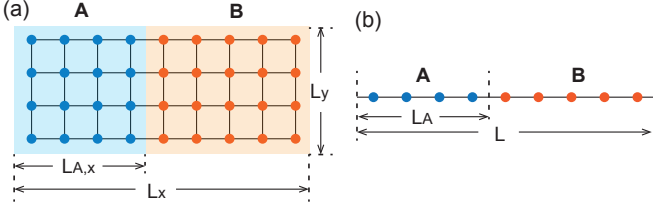


FIG. 1. Illustration of a system in (a) a 2D square lattice and (b) a 1D lattice divided into two subregions A and B.

For a given eigenstate $|\alpha\rangle$ of the entire region, we define the reduced density matrix in subregion A as

$$\rho_A(\alpha) = \text{tr}_B |\alpha\rangle\langle\alpha| = e^{-H_E^A(\alpha)}. \quad (3)$$

$H_E^A(\alpha)$ is known as the *entanglement Hamiltonian* [35] of eigenstate $|\alpha\rangle$. We define the eigenstate basis of the two subregion Hamiltonians by $H_A|\alpha_A, A\rangle = E_{\alpha_A}^A|\alpha_A, A\rangle$ and $H_B|\alpha_B, B\rangle = E_{\alpha_B}^B|\alpha_B, B\rangle$, where $E_{\alpha_A}^A$ and $E_{\alpha_B}^B$ are the eigenenergies ($1 \leq \alpha_A \leq N_A, 1 \leq \alpha_B \leq N_B$). If the eigenstate $|\alpha\rangle$ has wavefunction

$$|\alpha\rangle = \sum_{\alpha_A, \alpha_B} u_{\alpha, \alpha_A, \alpha_B} |\alpha_A, A\rangle \otimes |\alpha_B, B\rangle, \quad (4)$$

the elements of $\rho_A(\alpha)$ will be $\langle\alpha_A, A|\rho_A(\alpha)|\alpha'_A, A\rangle = \sum_{\alpha_B} u_{\alpha, \alpha_A, \alpha_B} u_{\alpha, \alpha'_A, \alpha_B}^*$. We now investigate the relation between the entanglement Hamiltonians of excited states and conserved quantities.

—*Fully chaotic systems.* For a many-body chaotic system without any (quasi)local conserved quantities besides the Hamiltonian, the ETH holds. As a sum of local terms obeying the ETH, H_{AB} in the basis $|\alpha_A, A\rangle \otimes |\alpha_B, B\rangle$ will have matrix elements $(H_{AB})_{\alpha'_A, \alpha'_B; \alpha_A, \alpha_B} = \delta_{\alpha_A, \alpha'_A} \delta_{\alpha_B, \alpha'_B} E^{(d)}(E_{\alpha_A}^A, E_{\alpha_B}^B) + h_{\alpha'_A, \alpha'_B; \alpha_A, \alpha_B}^{(\text{off})}$, where $h_{\alpha'_A, \alpha'_B; \alpha_A, \alpha_B}^{(\text{off})}$ is a random off-diagonal matrix decaying exponentially in $|E_{\alpha_A}^A - E_{\alpha'_A}^A|$ or $|E_{\alpha_B}^B - E_{\alpha'_B}^B|$ [16, 36]. When the boundary size $l_{AB} \ll L_A, L_B$, one can show that a typical excited state $|\alpha\rangle$ satisfies $u_{\alpha, \alpha_A, \alpha_B} u_{\alpha, \alpha'_A, \alpha'_B}^* \propto \delta_{\alpha_A, \alpha'_A} \delta_{\alpha_B, \alpha'_B} \delta(E_{\alpha} - E_{\alpha_A}^A - E_{\alpha_B}^B - E^{(d)})$ under the random average of $h^{(\text{off})}$ (supplementary material (SM) [36] Sec. S1), which determines the reduced density matrix $\rho_A(\alpha)$. The width of the delta function $\propto l_{AB}$, while generically $E_{\alpha_A}^A \propto L_A$, $E_{\alpha_B}^B \propto L_B$, and $E^{(d)} \propto l_{AB}$. We define $E_{av}^A = \text{tr}(H_A)/N_A$ and $E_{av} = \text{tr}(H)/N$ as the means of $E_{\alpha_A}^A$ and E_{α} . When $l_{AB} \ll L_A \ll L_B$, we can expand $\rho_A(\alpha)$ to the linear order of $E_{\alpha_A}^A - E_{av}^A$ and $\frac{l_{AB}}{L_A}$. This gives an entanglement Hamiltonian (up to subregion A boundary terms)

$$H_E^A(\alpha) \approx \beta_A^{(0)}(\alpha) I_A + \beta_A^{(1)}(\alpha) (H_A - E_{av}^A), \quad (5)$$

where $\beta_A^{(0)}(\alpha) = \log \left[\frac{N_A \Omega(E_{\alpha})}{\Omega_B(E_{\alpha} - E_{av}^A)} \right]$, and $\beta_A^{(1)}(\alpha) = (1 + \frac{E_{\alpha} - E_{av}}{\epsilon_0^{AB}} \frac{l_{AB}}{L_A L_B}) \frac{d \log \Omega_B(E)}{dE} \big|_{E=E_{\alpha} - E_{av}^A}$, with ϵ_0^{AB} of order 1.

Here $\Omega(E)$ and $\Omega_B(E)$ are the normalized densities of states of $H_A \otimes I_B + I_A \otimes H_B$ and H_B , respectively. This agrees with the ETH, which suggests that $H_E^A(\alpha)$ resembles the physical Hamiltonian H_A .

—*Generic systems and the EHSM.* A generic system may have multiple (quasi)local conserved quantities. We define $(Q, M) = \text{tr}(Q^\dagger M)$ as the *Frobenius (Hilbert-Schmidt) inner product* of operators Q and M , and $\|M\| = \sqrt{(M, M)}$ as the *Frobenius norm* of matrix M . A conserved quantity Q of a system with volume L is then defined as local or quasilocal if its overlap (Q, M_k) with any k -site locally supported product operator M_k is asymptotically constant as $L \rightarrow \infty$.

Assume a volume L quantum system has linearly independent Hermitian conserved quantities $Q^{(n)}$ ($n \geq 0$, not necessarily (quasi)local), which satisfy $[Q^{(m)}, Q^{(n)}] = [H, Q^{(n)}] = 0$. The Hamiltonian H is equal to some linear combination of $Q^{(n)}$. Without loss of generality, we define $Q^{(0)} = I$ as the identity matrix, and assume that $(Q^{(m)}, Q^{(n)}) = 0$ if $m \neq n$ (which indicates $\text{tr}(Q^{(n)}) = 0$ for $n \geq 1$). The energy eigenstates $|\alpha\rangle$ can thus also be chosen as eigenstates of $Q^{(n)}$, namely,

$$Q^{(n)}|\alpha\rangle = q_{\alpha}^{(n)}|\alpha\rangle. \quad (6)$$

Similar to Eq. (2), we can decompose each conserved quantity ($n \geq 1$) as

$$Q^{(n)} = Q_A^{(n)} \otimes I_B + I_A \otimes Q_B^{(n)} + Q_{AB}^{(n)}, \quad (7)$$

where $Q_A^{(n)} \otimes I_B$ ($I_A \otimes Q_B^{(n)}$) consists of product terms with supports in subregion A (B), while $Q_{AB}^{(n)}$ contains product terms with supports across subregions A and B.

If $Q^{(n)}$ is (quasi)local, one expects $Q_{AB}^{(n)}$ to be smaller than $Q_A^{(n)} \otimes I_B$ ($I_A \otimes Q_B^{(n)}$) by a factor $\frac{l_{AB}}{L_A}$ ($\frac{l_{AB}}{L_B}$). Thus, when $l_{AB} \ll L_A, L_B$, $Q_A^{(n)}$ and $Q_B^{(n)}$ are approximately conserved quantities in subregions A and B, which allows us to assume that the subregion energy eigenstates approximately satisfy $Q_A^{(n)}|\alpha_A, A\rangle = q_{A, \alpha_A}^{(n)}|\alpha_A, A\rangle$ and $Q_B^{(n)}|\alpha_B, B\rangle = q_{B, \alpha_B}^{(n)}|\alpha_B, B\rangle$. Statistically, we expect that $u_{\alpha, \alpha_A, \alpha_B} u_{\alpha, \alpha'_A, \alpha'_B}^* \propto \delta_{\alpha_A, \alpha'_A} \delta_{\alpha_B, \alpha'_B} \delta(q_{\alpha}^{(n)} - q_{A, \alpha_A}^{(n)} - q_{B, \alpha_B}^{(n)} - q_{\alpha_A, \alpha_B}^{(n, d)})$, where $q_{\alpha_A, \alpha_B}^{(n, d)}$ is the diagonal element of $Q_{AB}^{(n)}$ (SM [36] Sec. S2). In contrast, if $Q^{(n)}$ is nonlocal, one expects $Q_{AB}^{(n)}$ to be comparable to $Q_A^{(n)} \otimes I_B$ and $I_A \otimes Q_B^{(n)}$, so $Q_A^{(n)}$ and $Q_B^{(n)}$ are not approximate subregion conserved quantities, and $u_{\alpha, \alpha_A, \alpha_B}$ should barely depend on the $Q_A^{(n)}$ and $Q_B^{(n)}$ eigenvalues. Thus, similar to Eq. (5), when $l_{AB} \ll L_A \ll L_B$, we expect the subregion A entanglement Hamiltonian of typical excited states to be approximately (SM [36] Sec. S2, up to subregion A boundary terms)

$$H_E^A(\alpha) \approx \beta_A^{(0)}(\alpha) I_A + \sum_{n \in \text{Loc}} \beta_A^{(n)}(\alpha) Q_A^{(n)}, \quad (8)$$

where $n \in \text{Loc}$ runs over all the (quasi)local conserved quantities (excluding $n = 0$). The coefficients are approximately $\beta_A^{(n)}(\alpha) = b_\alpha^{(n)} \frac{d \log \Omega_B^{(n)}(q)}{dq} \big|_{q=q_\alpha^{(n)}}$ with $b_\alpha^{(n)} \rightarrow 1$ as $\frac{l_{AB}}{L_A} \rightarrow 0$, and $\beta_A^{(0)}(\alpha) = \log N_A + \sum_{n \in \text{Loc}} \log \frac{\Omega_B^{(n)}(q_\alpha^{(n)})}{\Omega_B^{(n)}(q_\alpha^{(n)})}$.

Here $\Omega_B^{(n)}(q_\alpha^{(n)})$ and $\Omega_B^{(n)}(q_B^{(n)})$ are the normalized density of states of $Q_A^{(n)} \otimes I_B + I_A \otimes Q_B^{(n)}$ and $Q_B^{(n)}$, respectively.

Eq. (8) allows the recovery of subregion (quasi)local conserved quantities $Q_A^{(n)}$ from the entanglement Hamiltonians. An entanglement Hamiltonian $H_E^A(\alpha)$ can be regarded as a vector $|H_E^A(\alpha)\rangle$ in the space of $N_A \times N_A$ matrices. Given the entanglement Hamiltonians of eigenstates α in an ensemble Ξ , we can define an *entanglement Hamiltonian superdensity matrix* (EHSM) of size $N_A^2 \times N_A^2$:

$$R_A = \sum_{\alpha \in \Xi} \frac{w_\alpha}{N_A} |H_E^A(\alpha)\rangle \langle H_E^A(\alpha)|, \quad (9)$$

where we assign a weight $w_\alpha > 0$ to each state $|\alpha\rangle$ ($\sum_{\alpha \in \Xi} w_\alpha = 1$). We can then diagonalize the EHSM R_A into

$$R_A = \sum_{n \geq 0} p_{A,n} |\bar{Q}_A^{(n)}\rangle \langle \bar{Q}_A^{(n)}|, \quad (10)$$

where $p_{A,n} \geq 0$ is the n -th eigenvalue ($n \geq 0$) of R_A (in descending order), and $\bar{Q}_A^{(n)}$ is the normalized eigenoperator satisfying $(\bar{Q}_A^{(m)}, \bar{Q}_A^{(n)}) = \text{tr}(\bar{Q}_A^{(m)\dagger} \bar{Q}_A^{(n)}) = \delta_{mn}$. We expect $\bar{Q}_A^{(n)}$ with large $p_{A,n}$ to resemble the normalized (quasi)local conserved quantities in subregion A . An extensive (quasi)local conserved quantity $Q_A^{(n)}$ in physical units will scale as $Q_A^{(n)} \sim \sqrt{N_A L_A} \bar{Q}_A^{(n)}$.

We note that if the ensemble Ξ contains $N_\Xi \ll N_A^2$ eigenstates, R_A can be efficiently diagonalized by diagonalizing a $N_\Xi \times N_\Xi$ correlation matrix $[S_A]_{\alpha\beta} = \frac{\sqrt{w_\alpha w_\beta}}{N_A} (H_E^A(\alpha), H_E^A(\beta))$ (see SM [36] Sec. S3). We now study the EHSM of several models below.

Free fermions. Free fermion models are many-body integrable by solving the single-particle spectra. We consider the Anderson model [25] in both a 2D square lattice and a 1D lattice as shown in Fig. 1, with Hamiltonian

$$H = -t \sum_{\langle ij \rangle} (c_{\mathbf{r}_i}^\dagger c_{\mathbf{r}_j} + h.c.) + \sum_j \mu_j c_{\mathbf{r}_j}^\dagger c_{\mathbf{r}_j}, \quad (11)$$

where t (real) is the nearest neighbor hopping, μ_j is an on-site random potential within an interval $[-W, W]$, and periodic boundary condition is imposed. Generically, the entanglement Hamiltonian of free fermions takes the form $H_E^A(\alpha) = \gamma_A(\alpha) I_A + \sum_{ij \in A} \kappa_{A,ij}(\alpha) c_{\mathbf{r}_i}^\dagger c_{\mathbf{r}_j}$ [36, 37].

For fixed system volume $L = 600$ ($L = 500$) and different A subregion volumes $L_A = 50, 100, 150$ ($L_A = 10, 30, 50$) in 2D (1D), we diagonalize the EHSM of an ensemble Ξ of $N_\Xi = 1000$ randomly chosen many-body eigenstates of model (11), with weight $w_\alpha = \frac{1}{N_\Xi}$. Fig.

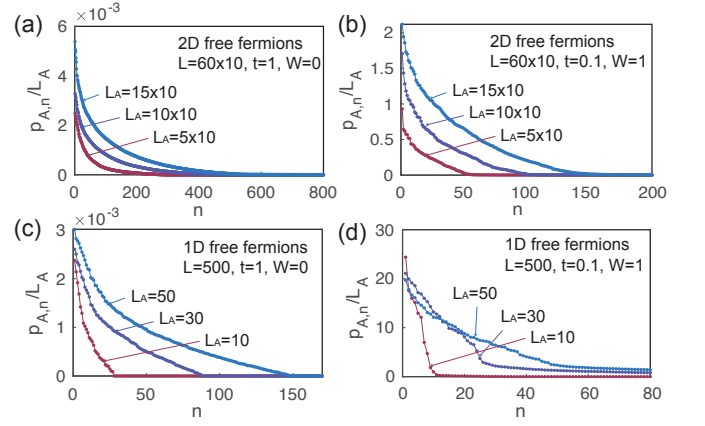


FIG. 2. The EHSM eigenvalues $p_{A,n}$ for free fermions (parameters given in the panels), calculated for $N_\Xi = 1000$ randomly chosen eigenstates. The model is on (see Fig. 1) (a)-(b) a 2D square lattice with total size $L_x = 60$, $L_y = 10$, $L = L_x L_y = 600$ and A subregion volume $L_A = L_{A,x} L_{A,y} = 50, 100, 150$; (c)-(d) a 1D lattice with total size $L = 500$ and A subregion size $L_A = 10, 30, 50$.

2(a) and (c) shows the results for $t = 1$ and $W = 0$ in 2D and 1D, where the single-fermion wavefunctions are extended. We find $p_{A,n}$ drops to zero around $n = 3L_A$. The eigen-operators $\bar{Q}_A^{(n)}$ of these $3L_A$ nonzero $p_{A,n}$ approximately give the linear combinations of conserved quantities I_A , $T_{x,y}^A = \sum_i (c_{x_i+x, y_i+y}^\dagger c_{x_i, y_i} + c_{x_i, y_i+y}^\dagger c_{x_i+x, y_i})$ and $P_{x,y}^A = \sum_i c_{x-x_i, y_i+y}^\dagger c_{x_i, y_i}$ (in 1D $y_i \equiv y \equiv 0$), as expected for subregion A with open (periodic) boundary condition in the x (y) direction (see SM [36] Sec. S4). In particular, $\bar{Q}_A^{(0)} \approx I_A / \sqrt{N_A}$. Fig. 2(b) and (d) show the cases with strong disorders W , where all single-particle eigenstates are strongly localized, and $p_{A,n}$ drops significantly towards zero around $n = L_A$. Accordingly, we find $\bar{Q}_A^{(0)} \approx I_A / \sqrt{N_A}$, and $\bar{Q}_A^{(n)}$ ($0 < n < L_A$) are approximately linear combinations of the occupation numbers of L_A localized single-particle eigenstates (SM [36] Sec. S4).

The XYZ model. As an example of interacting many-body systems, we study the traceless 1D XYZ model Hamiltonian in a magnetic field (with periodic boundary condition):

$$H = \sum_{j=1}^L \left[\sum_{\nu=x,y,z} J_\nu \sigma_{j,\nu} \sigma_{j+1,\nu} + (\mathbf{B} + \delta \mathbf{B}_j) \cdot \boldsymbol{\sigma}_j \right], \quad (12)$$

where $\sigma_{j,\nu}$ are the spin Pauli matrices on site j , J_ν are the neighboring spin interactions, \mathbf{B} is a uniform magnetic field, and $\delta \mathbf{B}_j$ is a random magnetic field with components $\delta B_{j,\nu} \in [-B_{R,\nu}, B_{R,\nu}]$ ($\nu = x, y, z$). We perform exact diagonalization of the model for $L = 14$ sites, and study the EHSMs of subregion A with $L_A \leq 7$ (Fig. 1(b), see SM [36] Sec. S5 for details).

In Fig. 3, we calculate the EHSM eigenvalues $p_{A,n}$ for

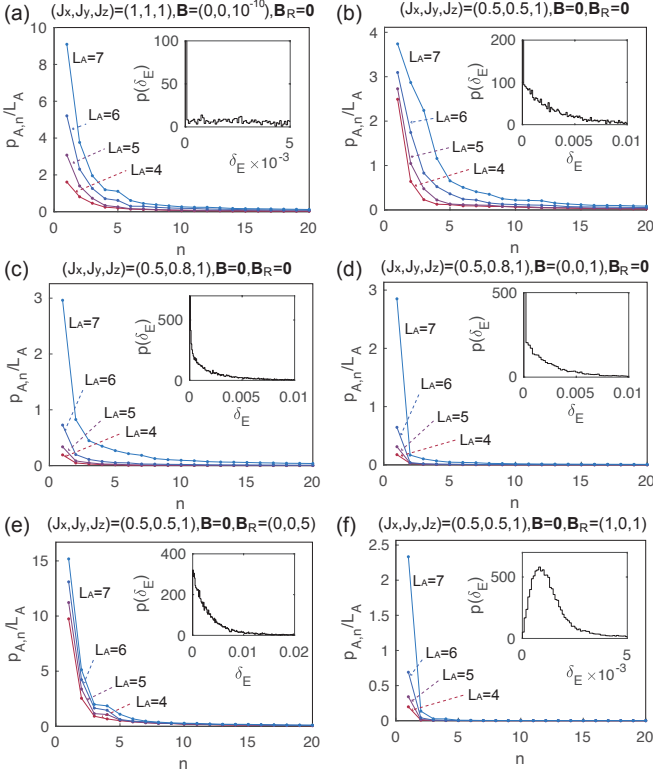


FIG. 3. The EHSM eigenvalues $p_{A,n}$ of the 1D XYZ model in a magnetic field, which are calculated for the ensemble Ξ of all the eigenstates $|\alpha\rangle$ with equal weights w_α . The full system size is $L = 14$, and the subregion size L_A and model parameters are given in each panel. The insets show the LSS of ensemble Ξ (Poisson in (a)-(e), and Wigner-Dyson in (f)).

the ensemble Ξ of all the N eigenstates $|\alpha\rangle$ with equal weights $w_\alpha = \frac{1}{N}$, with the parameters labeled in each panel. The insets show the LSS of the ensemble Ξ . The largest eigenvalue $p_{A,0}$ is not shown, which always dominantly gives $\overline{Q}_A^{(0)} \approx I_A/\sqrt{N_A}$. In Fig. 3(a)-(c) where $\mathbf{B} = \mathbf{B}_R = \mathbf{0}$, the XYZ model is exactly solvable [38, 39], and we find the EHSM eigenvalues approximately decaying as $p_{A,n} \propto n^{-s}$, with the exponent $s \approx 1$ (see SM [36] Fig. 7). For the XYZ model (three J_ν unequal) in a uniform magnetic field \mathbf{B} shown in Fig. 3(d), $p_{A,n}$ also decays approximately as n^{-s} (for $n > 2$) with $s \approx 1$, suggesting the existence of quasilocal conserved quantities, although local conserved quantities are proved non-existing [40]. Fig. 3(e) shows the EHSM of XXZ model ($J_x = J_y \neq J_z$) with a \hat{z} direction random field \mathbf{B}_R , which is in the many-body localization (MBL) phase [26–30]. In this case, we also find approximately $p_{A,n} \propto n^{-s}$, but with a larger $s \approx 1.5 \sim 2$ (SM [36] Sec. S5A). We expect the eigen-operators to give the MBL localized conserved quantities [31–34], which makes the system (approximately) integrable. We note that the power-law decaying $p_{A,n}$ of the integrable XYZ models (which may be subject to finite size effects) is different from the sharp

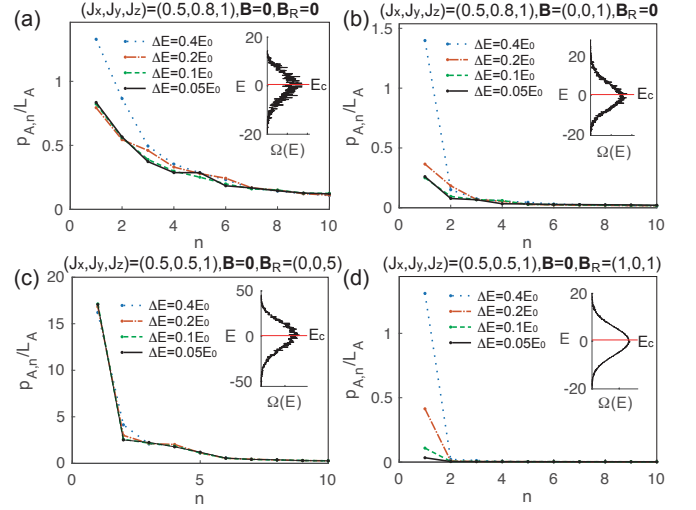


FIG. 4. The EHSM eigenvalues $p_{A,n}$ ($n \geq 1$) of the 1D XYZ model for an ensemble Ξ of all eigenstates in the energy interval $[E_c - \frac{\Delta E}{2}, E_c + \frac{\Delta E}{2}]$, where ΔE is varied. The full system (subregion) size is $L = 14$ ($L_A = 7$). E_0 is the range of the energy spectrum of the entire system. The insets show the density of states $\Omega(E)$ of the system and E_c .

cutoff of nonzero $p_{A,n}$ of the free fermions in Fig. 2. Lastly, for the XXZ model with a random direction field \mathbf{B}_R shown in Fig. 3(f), the LLS shows the Wigner-Dyson distribution, indicating full quantum chaos. In this case, only $p_{A,0}$ and $p_{A,1}$ are significantly nonzero, which correspond to linear combinations of the only two local conserved quantities I_A and H_A , in agreement with ETH (Eq. (5)).

We now take a closer look at the eigen-operators $\overline{Q}_A^{(n)}$ of the EHSM, which well commute with subregion Hamiltonian H_A for small n (SM [36] Sec. S5B). We find the eigen-operator of the largest eigenvalue $p_{A,0}$ is generically quite accurately $\overline{Q}_A^{(0)} \propto I_A$. In Fig. 3(a),(b),(e) which possess a \hat{z} direction spin rotational symmetry, $\overline{Q}_A^{(1)}$ and $\overline{Q}_A^{(2)}$ are approximately linear combinations of H_A and $\sum_j \sigma_{j,z}$ (SM [36] Tab. S2). In the Fig. 3(c),(d),(f) cases, we find dominantly $\overline{Q}_A^{(1)} \propto H_A$. The higher eigen-operators $\overline{Q}_A^{(n)}$ are generically more complicated and less local (SM [36] Sec. S5C). In the zero field XXZ model (Fig. 3(a),(b)), we find $\overline{Q}_A^{(3)} \approx \sum_{j,\ell,\nu} \zeta_\nu(l) \sigma_{\nu,j} \sigma_{\nu,j+l} + \zeta' \sum_j \sigma_{z,j}$, with the functions $\zeta_\nu(l)$ decaying with l , and ζ' being some constant. $\overline{Q}_A^{(4)}$ has a large overlap with the known support-4 local conserved quantity P_4 of XXZ model [6, 7] (SM [36] Sec. S5C). However, we find the known support-3 local conserved quantity P_3 [6, 7] has zero overlap with all $\overline{Q}_A^{(n)}$.

We can also calculate the EHSM for a microcanonical ensemble Ξ consisting of all the eigenstates $|\alpha\rangle$ with energies $E_\alpha \in [E_c - \frac{\Delta E}{2}, E_c + \frac{\Delta E}{2}]$ with equal weights w_α , for

some energy E_c , to characterize the integrability at energy E_c . Fig. 4 (a)-(c) show the cases with (quasi)local conserved quantities other than I_A and H_A , where the nonzero EHS eigenvalues $p_{A,n}$ ($n \geq 1$) asymptotically approach nonzero constants as $\Delta E \rightarrow 0$. In sharp contrast, in the fully chaotic case where the ETH holds, we find $p_{A,n} \rightarrow 0$ for all $n \geq 1$ when $\Delta E \rightarrow 0$. This is because all the entanglement Hamiltonians are given by Eq. (5) with $E_\alpha = E_c$ and thus equal, leading to only one nonzero EHS eigenvalue $p_{A,0}$ and the corresponding eigen-operator $\bar{Q}_A^{(0)} \propto \beta_A^{(0)} I_A + \beta_A^{(1)} H_A$.

Discussion. We have shown that the (quasi)local subregion conserved quantities can be recovered as eigenoperators of the EHS of the entanglement Hamiltonians of an ensemble of excited eigenstates, with their EHS eigenvalues $p_{A,n} > 0$. For free fermions, we find nonzero $p_{A,n}$ shows a cutoff around the order of the subsystem volume. For the interacting XYZ model, if the system is integrable, within the system sizes calculable, $p_{A,n}$ decay approximately as n^{-s} , with $s \approx 1$ ($s \approx 1.5 \sim 2$) if the system is delocalized (MBL). For fully chaotic sys-

tems, only $p_{A,0}$ and $p_{A,1}$ are significantly nonzero, the eigen-operators of which correspond to the identity I_A and the subregion Hamiltonian H_A . We conjecture that the conserved quantities from EHS with large $p_{A,n}$ govern the integrability of a system: they allow prediction of a system's evolution from subregion observables, without knowing the entire wavefunction. Not all the (quasi)local conserved quantities appear in the EHS, for instance, the conserved quantity P_3 in the XXZ model is absent. Open future questions await, such as the decaying behaviors of EHS eigenvalues of generic integrable systems at large system sizes, and how the EHS eigen-operators affect the nonequilibrium thermodynamics.

ACKNOWLEDGMENTS

Acknowledgments. The author is grateful to conversations with Yichen Hu, Abhinav Prem, and especially the insightful discussion with David Huse.

-
- [1] Marcos Rigol, Vanja Dunjko, Vladimir Yurovsky, and Maxim Olshanii, "Relaxation in a completely integrable many-body quantum system: An ab initio study of the dynamics of the highly excited states of 1d lattice hardcore bosons," *Phys. Rev. Lett.* **98**, 050405 (2007).
 - [2] Marcos Rigol, Vanja Dunjko, and Maxim Olshanii, "Thermalization and its mechanism for generic isolated quantum systems," *Nature* **452**, 854–858 (2008).
 - [3] Jean-Sébastien Caux and Robert M. Konik, "Constructing the generalized gibbs ensemble after a quantum quench," *Phys. Rev. Lett.* **109**, 175301 (2012).
 - [4] Jean-Sébastien Caux and Fabian H. L. Essler, "Time evolution of local observables after quenching to an integrable model," *Phys. Rev. Lett.* **110**, 257203 (2013).
 - [5] Lev Vidmar and Marcos Rigol, "Generalized gibbs ensemble in integrable lattice models," *Journal of Statistical Mechanics: Theory and Experiment* **2016**, 064007 (2016).
 - [6] M. G. Tetelman, "Lorentz group for two-dimensional integrable lattice systems," *Sov. Phys. JETP* **55**, 306 (1981).
 - [7] M.P. Grabowski and P. Mathieu, "Structure of the conservation laws in quantum integrable spin chains with short range interactions," *Annals of Physics* **243**, 299–371 (1995).
 - [8] Enej Ilievski, Marko Medenjak, and Tomaž Prosen, "Quasilocal conserved operators in the isotropic heisenberg spin-1/2 chain," *Phys. Rev. Lett.* **115**, 120601 (2015).
 - [9] Yuji Nozawa and Kouhei Fukai, "Explicit construction of local conserved quantities in the XYZ spin-1/2 chain," *Phys. Rev. Lett.* **125**, 090602 (2020).
 - [10] Michael Victor Berry, M. Tabor, and John Michael Ziman, "Level clustering in the regular spectrum," *Proceedings of the Royal Society of London. A. Mathematical and Physical Sciences* **356**, 375–394 (1977), <https://royalsocietypublishing.org/doi/pdf/10.1098/rspa.1977.0140>.
 - [11] O. Bohigas, M. J. Giannoni, and C. Schmit, "Characterization of chaotic quantum spectra and universality of level fluctuation laws," *Phys. Rev. Lett.* **52**, 1–4 (1984).
 - [12] R. V. Jensen and R. Shankar, "Statistical behavior in deterministic quantum systems with few degrees of freedom," *Phys. Rev. Lett.* **54**, 1879–1882 (1985).
 - [13] J. M. Deutsch, "Quantum statistical mechanics in a closed system," *Phys. Rev. A* **43**, 2046–2049 (1991).
 - [14] Mark Srednicki, "Chaos and quantum thermalization," *Phys. Rev. E* **50**, 888–901 (1994).
 - [15] Mark Srednicki, "The approach to thermal equilibrium in quantized chaotic systems," *Journal of Physics A: Mathematical and General* **32**, 1163–1175 (1999).
 - [16] Luca D'Alessio, Yariv Kafri, Anatoli Polkovnikov, and Marcos Rigol, "From quantum chaos and eigenstate thermalization to statistical mechanics and thermodynamics," *Advances in Physics* **65**, 239–362 (2016), <https://doi.org/10.1080/00018732.2016.1198134>.
 - [17] Juan Maldacena, Stephen H. Shenker, and Douglas Stanford, "A bound on chaos," *Journal of High Energy Physics* **2016** (2016), 10.1007/jhep08(2016)106.
 - [18] Subir Sachdev and Jinwu Ye, "Gapless spin fluid ground state in a random, quantum Heisenberg magnet," *Phys. Rev. Lett.* **70**, 3339 (1993), arXiv:cond-mat/9212030 [cond-mat].
 - [19] Joseph Polchinski and Vladimir Rosenhaus, "The Spectrum in the Sachdev-Ye-Kitaev Model," *JHEP* **04**, 001 (2016), arXiv:1601.06768 [hep-th].
 - [20] Juan Maldacena and Douglas Stanford, "Remarks on the Sachdev-Ye-Kitaev model," *Phys. Rev. D* **94**, 106002 (2016), arXiv:1604.07818 [hep-th].
 - [21] Alexei Kitaev and S. Josephine Suh, "The soft mode in the Sachdev-Ye-Kitaev model and its gravity dual," *JHEP* **05**, 183 (2018), arXiv:1711.08467 [hep-th].
 - [22] Biao Lian, S. L. Sondhi, and Zhenbin Yang, "The chiral

- syk model,” *Journal of High Energy Physics* **2019** (2019), 10.1007/jhep09(2019)067.
- [23] Xiao-Liang Qi and Daniel Ranard, “Determining a local hamiltonian from a single eigenstate,” *Quantum* **3**, 159 (2019).
- [24] James R. Garrison and Tarun Grover, “Does a single eigenstate encode the full hamiltonian?” *Phys. Rev. X* **8**, 021026 (2018).
- [25] P. W. Anderson, “Absence of diffusion in certain random lattices,” *Phys. Rev.* **109**, 1492–1505 (1958).
- [26] D.M. Basko, I.L. Aleiner, and B.L. Altshuler, “Metal-insulator transition in a weakly interacting many-electron system with localized single-particle states,” *Annals of Physics* **321**, 1126–1205 (2006).
- [27] I. V. Gornyi, A. D. Mirlin, and D. G. Polyakov, “Interacting electrons in disordered wires: Anderson localization and low- t transport,” *Phys. Rev. Lett.* **95**, 206603 (2005).
- [28] Vadim Oganesyan and David A. Huse, “Localization of interacting fermions at high temperature,” *Phys. Rev. B* **75**, 155111 (2007).
- [29] Marko Žnidarič, Tomaž Prosen, and Peter Prelovšek, “Many-body localization in the heisenberg xxz magnet in a random field,” *Phys. Rev. B* **77**, 064426 (2008).
- [30] Arijeet Pal and David A. Huse, “Many-body localization phase transition,” *Phys. Rev. B* **82**, 174411 (2010).
- [31] Maksym Serbyn, Z. Papić, and Dmitry A. Abanin, “Local conservation laws and the structure of the many-body localized states,” *Phys. Rev. Lett.* **111**, 127201 (2013).
- [32] David A. Huse, Rahul Nandkishore, and Vadim Oganesyan, “Phenomenology of fully many-body-localized systems,” *Phys. Rev. B* **90**, 174202 (2014).
- [33] Anushya Chandran, Isaac H. Kim, Guifre Vidal, and Dmitry A. Abanin, “Constructing local integrals of motion in the many-body localized phase,” *Phys. Rev. B* **91**, 085425 (2015).
- [34] V. Ros, M. Müller, and A. Scardicchio, “Integrals of motion in the many-body localized phase,” *Nuclear Physics B* **891**, 420–465 (2015).
- [35] Hui Li and F. D. M. Haldane, “Entanglement spectrum as a generalization of entanglement entropy: Identification of topological order in non-abelian fractional quantum hall effect states,” *Phys. Rev. Lett.* **101**, 010504 (2008).
- [36] See Supplemental Material for details.
- [37] Ingo Peschel, “Calculation of reduced density matrices from correlation functions,” *Journal of Physics A: Mathematical and General* **36**, L205–L208 (2003).
- [38] Rodney Baxter, “Eight-vertex model in lattice statistics and one-dimensional anisotropic heisenberg chain. i. some fundamental eigenvectors,” *Annals of Physics* **76**, 1–24 (1973).
- [39] Rodney Baxter, “Eight-vertex model in lattice statistics and one-dimensional anisotropic heisenberg chain. ii. equivalence to a generalized ice-type lattice model,” *Annals of Physics* **76**, 25–47 (1973).
- [40] Naoto Shiraishi, “Proof of the absence of local conserved quantities in the XYZ chain with a magnetic field,” *EPL (Europhysics Letters)* **128**, 17002 (2019).

SUPPLEMENTARY MATERIAL FOR “CONSERVED QUANTITIES FROM ENTANGLEMENT HAMILTONIAN”

CONTENTS

Acknowledgments	5
References	5
Supplementary Material for “Conserved Quantities from Entanglement Hamiltonian”	6
S1. Entanglement Hamiltonian of a fully chaotic system	7
A. Estimation of the boundary term H_{AB} from ETH	7
B. Derivation of the entanglement Hamiltonian for eigenstates	8
C. The case when the Hamiltonian is extremely nonlocal	10
S2. Entanglement Hamiltonian of systems with multiple conserved quantities	10
S3. Diagonalization of the EHSM	12
S4. The EHSM of free fermions	13
A. Numerical results	14
1. Extended fermions	15
2. Localized fermions	16
S5. The EHSM of the 1D XYZ model in a magnetic field	17
A. EHSM eigenvalues and entanglement entropies	17
B. How well the EHSM eigen-operators are conserved quantities	19

S1. ENTANGLEMENT HAMILTONIAN OF A FULLY CHAOTIC SYSTEM

In this section, we study the properties of eigenstate wavefunctions of the Hamiltonian in main text Eq. (2) when the system is fully quantum chaotic. The $N \times N$ Hamiltonian (N : Hilbert space dimension of the full system) in the main text Eq. (2) is of the form:

$$H = H_0 + H_{AB}, \quad H_0 = H_A \otimes I_B + I_A \otimes H_B. \quad (13)$$

Here the subregions A and B have sizes (number of sites) L_A and L_B , respectively, and the total number of sites is $L = L_A + L_B$. Besides, we denote the number of sites on the boundary between subregions A and B as l_{AB} .

For a local Hamiltonian and $l_{AB} \ll L_A, L_B$ (i.e., large system sizes), H_0 is dominant, and H_{AB} can be treated as a perturbation. We adopt the subregion eigenstate direct product basis $|\alpha_A, A; \alpha_B, B\rangle = |\alpha_A, A\rangle \otimes |\alpha_B, B\rangle$, where $H_A|\alpha_A, A\rangle = E_{\alpha_A}^A|\alpha_A, A\rangle$ and $H_B|\alpha_B, B\rangle = E_{\alpha_B}^B|\alpha_B, B\rangle$ ($1 \leq \alpha_A \leq N_A$, $1 \leq \alpha_B \leq N_B$, with $N_A = d^{L_A}$, $N_B = d^{L_B}$ being the Hilbert space dimensions of subregions A and B , $N_A N_B = N$). In this basis, both H_A and H_B are diagonal, and thus H_0 is diagonal, with eigenvalues $E_{\alpha_A}^A + E_{\alpha_B}^B$.

A. Estimation of the boundary term H_{AB} from ETH

If the system is fully quantum chaotic, one expects ETH to hold. Since the Hamiltonian is local, we expect

$$H_{AB} = \sum_m \mathcal{O}_m^A \mathcal{O}_m^B \quad (14)$$

is the sum over a set of local terms $\mathcal{O}_m^A \mathcal{O}_m^B$, where \mathcal{O}_m^A is supported in subregion A and \mathcal{O}_m^B is supported in subregion B . The number of m indices is proportional to the boundary size l_{AB} . According to ETH [12–16], their matrix elements can be estimated as

$$\begin{aligned} \langle \alpha'_A, A | \mathcal{O}_m^A | \alpha_A, A \rangle &= O_m^A(\bar{E}_A) \delta_{\alpha_A, \alpha'_A} + e^{-S_A(\bar{E}_A)/2} f_m^A(\bar{E}_A, \omega_A) r_{\alpha_A, \alpha'_A}^{A, m}, \\ \langle \alpha'_B, B | \mathcal{O}_m^B | \alpha_B, B \rangle &= O_m^B(\bar{E}_B) \delta_{\alpha_B, \alpha'_B} + e^{-S_B(\bar{E}_B)/2} f_m^B(\bar{E}_B, \omega_B) r_{\alpha_B, \alpha'_B}^{B, m}, \end{aligned} \quad (15)$$

where $\bar{E}_A = (E_{\alpha_A}^A + E_{\alpha'_A}^A)/2$ and $\bar{E}_B = (E_{\alpha_B}^B + E_{\alpha'_B}^B)/2$ are the average energies, $\omega_A = E_{\alpha_A}^A - E_{\alpha'_A}^A$ and $\omega_B = E_{\alpha_B}^B - E_{\alpha'_B}^B$ are energy differences, while $S_A(\bar{E}_A)$ and $S_B(\bar{E}_B)$ are the entropies in each subregion at the average energies. $r_{\alpha_A, \alpha'_A}^{A, m}$ and $r_{\alpha_B, \alpha'_B}^{B, m}$ are random matrices with a root mean square for each element being 1. We note that for chaotic systems satisfying the ETH, $e^{-S_A(\bar{E}_A)/2} \propto 1/\sqrt{N_A}$, and $e^{-S_B(\bar{E}_B)/2} \propto 1/\sqrt{N_B}$. The function $f_m^{A, B}(E, \omega)$ decay exponentially as $e^{-|\omega|/\omega_0}$ at large ω (comparable to ω_0), and is smooth at small ω (the values scale as \sqrt{L}), where ω_0 is independent of system size (i.e., of order 1 in the expansion with respect to system size $L_{A, B}$) [16]. Therefore, we find H_{AB} (contributed by order l_{AB} number of local terms $\mathcal{O}_m^A \mathcal{O}_m^B$) under the basis $|\alpha_A, A\rangle \otimes |\alpha_B, B\rangle$ consists of a diagonal part and an off-diagonal part:

$$\begin{aligned} H_{AB} &= H_{AB}^{(d)} + h^{(\text{off})}, \\ (H_{AB}^{(d)})_{\alpha'_A \alpha'_B; \alpha_A \alpha_B} &= \delta_{\alpha_A, \alpha'_A} \delta_{\alpha_B, \alpha'_B} E^{(d)}(E_{\alpha_A}^A, E_{\alpha_B}^B), \\ h_{\alpha'_A \alpha'_B; \alpha_A \alpha_B}^{(\text{off})} &= \delta_{\alpha_A, \alpha'_A} r_{\alpha_B, \alpha'_B}^B \frac{\lambda_B(\bar{E}_B, \omega_B)}{\sqrt{N_B}} + \delta_{\alpha_B, \alpha'_B} r_{\alpha_A, \alpha'_A}^A \frac{\lambda_A(\bar{E}_A, \omega_A)}{\sqrt{N_A}} + \frac{\lambda_{AB}(\bar{E}_A, \omega_A, \bar{E}_B, \omega_B)}{\sqrt{N}} r_{\alpha_A \alpha_B, \alpha'_A \alpha'_B}^{AB}, \end{aligned} \quad (16)$$

where all the r matrices are random matrices with the root mean square of each element being 1, while the functions $\lambda_A, \lambda_B, \lambda_{AB}$ are proportional to $\sqrt{L_A l_{AB}}, \sqrt{L_B l_{AB}}, \sqrt{L_A L_B l_{AB}}$ and decay as $e^{-|\omega_A|/\omega_{A,0}}, e^{-|\omega_B|/\omega_{B,0}}$ and $e^{-|\omega_A|/\omega_{A,0} - |\omega_B|/\omega_{B,0}}$, with $\omega_{A,0}$ and $\omega_{B,0}$ independent of system sizes L_A and L_B . To the lowest order, we can approximately assume the diagonal part takes the form of

$$E^{(d)}(E_{\alpha_A}^A, E_{\alpha_B}^B) \approx \frac{l_{AB}}{\epsilon_0^{AB}} \left(\frac{E_{\alpha_A}^A}{L_A} - \epsilon_0^A \right) \left(\frac{E_{\alpha_B}^B}{L_B} - \epsilon_0^B \right), \quad (17)$$

where l_{AB} is the boundary area (number of sites on the boundary), while ϵ_0^{AB} , ϵ_0^A and ϵ_0^B are of order 1 energies and are asymptotically independent of system sizes L_A and L_B . Since we have defined that each product term in the boundary term H_{AB} is traceless, we have

$$\epsilon_0^A = \frac{1}{N_A L_A} \sum_{\alpha_A=1}^{N_A} E_{\alpha_A}^A = \frac{E_{av}^A}{L_A}, \quad \epsilon_0^B = \frac{1}{N_B L_B} \sum_{\alpha_B=1}^{N_B} E_{\alpha_B}^B = \frac{E_{av}^B}{L_B}, \quad (18)$$

where E_{av}^A and E_{av}^B are the mean values of $E_{\alpha_A}^A$ and $E_{\alpha_B}^B$, respectively. Note that for systems with delocalized eigenstates (e.g., the fully chaotic systems considered here), the energy range of $E_{\alpha_A}^A$ ($E_{\alpha_B}^B$) generically scale linearly with L_A (L_B), so ϵ_0^A and ϵ_0^B are of order 1.

This yields a correlation for the matrix elements of the off-diagonal Hermitian part h^{off} (averaged over the random r matrices in Eq. (16)):

$$\langle h_{\alpha'_A \alpha'_B; \alpha_A \alpha_B}^{\text{off}} \rangle = 0, \quad \langle h_{\alpha'_A \alpha'_B; \alpha_A \alpha_B}^{\text{off}} h_{\alpha_A \alpha_B; \alpha'_A \alpha'_B}^{\text{off}} \rangle = \frac{\lambda_{AB}^2}{N} + \delta_{\alpha_A, \alpha'_A} \frac{\lambda_B^2}{N_B} + \delta_{\alpha_B, \alpha'_B} \frac{\lambda_A^2}{N_A}, \quad (19)$$

where we have omitted the variables of the functions λ_{AB} , λ_A and λ_B for simplicity. Note that here the bra and ket stands for the average over the random r matrices in Eq. (16).

B. Derivation of the entanglement Hamiltonian for eigenstates

To find the properties of the eigenstate wavefunctions for determining the entanglement Hamiltonian, we treat the off-diagonal part h^{off} of H_{AB} as fluctuating quantum fields obeying Eq. (19), and define the statistically averaged Green's function:

$$G_{\alpha_A \alpha_B; \alpha'_A \alpha'_B}(\omega) = \left\langle \left(\langle \alpha_A, A; \alpha_B, B | \frac{1}{\omega - H} | \alpha'_A, A; \alpha'_B, B \rangle \right) \right\rangle = \delta_{\alpha_A \alpha'_A} \delta_{\alpha_B \alpha'_B} G_{\alpha_A \alpha_B}(\omega), \quad (20)$$

where the outer bra and ket stand for the statistical average over all possible random h^{off} matrices satisfying Eq. (19). The fact that $G_{\alpha_A \alpha_B; \alpha'_A \alpha'_B}(\omega) \propto \delta_{\alpha_A \alpha'_A} \delta_{\alpha_B \alpha'_B}$ can be seen by noting that $G_{\alpha_A \alpha_B; \alpha'_A \alpha'_B}(\omega)$ should be invariant under flipping of any basis $|\alpha_A, A\rangle \rightarrow -|\alpha_A, A\rangle$ or $|\alpha_B, B\rangle \rightarrow -|\alpha_B, B\rangle$, given that the matrix elements of h^{off} are random with zero mean. In the large N_A, N_B limit, by treating h^{off} as a matrix quantum field, one can show that the Green's function $G_{\alpha_A \alpha_B}(\omega)$ satisfy the Schwinger-Dyson (SD) equation:

$$G_{0, \alpha_A \alpha_B}(\omega)^{-1} = G_{\alpha_A \alpha_B}(\omega)^{-1} + \Sigma_{\alpha_A \alpha_B}(\omega), \quad (21)$$

where the unperturbed Green's function $G_{0, \alpha_A \alpha_B}(\omega)$ and the self energy $\Sigma_{\alpha_A \alpha_B}(\omega)$ are given by

$$G_{0, \alpha_A \alpha_B}(\omega) = \frac{1}{\omega - E_{\alpha_A}^A - E_{\alpha_B}^B - E^{(d)}(E_{\alpha_A}^A, E_{\alpha_B}^B)}, \quad \Sigma_{\alpha_A \alpha_B}(\omega) = \sum_{\alpha'_A \alpha'_B} \langle h_{\alpha'_A \alpha'_B; \alpha_A \alpha_B}^{\text{off}} h_{\alpha_A \alpha_B; \alpha'_A \alpha'_B}^{\text{off}} \rangle G_{\alpha'_A \alpha'_B}(\omega). \quad (22)$$

Eqs. (21) and (22) then gives a self-consistent equation

$$\Sigma_{\alpha_A \alpha_B}(\omega) = \frac{1}{N} \sum_{\alpha'_A \alpha'_B} \frac{\lambda_{AB}^2 + N_A \lambda_B^2 \delta_{\alpha_A, \alpha'_A} + N_B \lambda_A^2 \delta_{\alpha_B, \alpha'_B}}{\omega - E_{\alpha'_A}^A - E_{\alpha'_B}^B - E^{(d)}(E_{\alpha'_A}^A, E_{\alpha'_B}^B) - \Sigma_{\alpha'_A \alpha'_B}(\omega)}. \quad (23)$$

In the large L_A and L_B limit, h^{off} is much smaller than H_A and H_B , thus Eq. (22) implies that the self energy $\Sigma_{\alpha_A \alpha_B}(\omega)$ is much smaller than $E_{\alpha'_A}^A$ and $E_{\alpha'_B}^B$. To the leading order of $\frac{l_{AB}}{L_A}$ and $\frac{l_{AB}}{L_B}$, ignoring the $E^{(d)}(E_{\alpha'_A}^A, E_{\alpha'_B}^B)$ and $\Sigma_{\alpha'_A \alpha'_B}(\omega)$ term in the denominator, and turn the summation over α'_A, α'_B into an integration, we find an imaginary self energy

$$\begin{aligned} \Sigma_{\alpha_A \alpha_B}(\omega) \approx & 2\pi i \left[\left(\int dE^A \Omega_A(E^A) \Omega_B(\omega - E^A) \lambda_{AB}^2 \left(\frac{E_{\alpha_A}^A + E^A}{2}, E_{\alpha_A}^A - E^A, \frac{E_{\alpha_B}^B + \omega - E^A}{2}, E_{\alpha_B}^B - \omega + E^A \right) \right) \right. \\ & \left. + \Omega_B(\omega - E_{\alpha_A}^A) \lambda_B^2(E_{\alpha_B}^B, 0) + \Omega_A(\omega - E_{\alpha_B}^B) \lambda_A^2(E_{\alpha_A}^A, 0) \right], \end{aligned} \quad (24)$$

where we have defined

$$\Omega_A(E) = \frac{1}{N_A} \sum_{\alpha_A} \delta(E - E_{\alpha_A}^A), \quad \Omega_B(E) = \frac{1}{N_B} \sum_{\alpha_B} \delta(E - E_{\alpha_B}^B) \quad (25)$$

as the normalized density of states in subregions A and B ($\int \Omega_A(E) dE = \int \Omega_B(E) dE = 1$). Note that since the range of energies in subregions A (B) is proportional to L_A (L_B), we have $\Omega_A(E) \propto 1/L_A$ and $\Omega_B(E) \propto 1/L_B$. Therefore, we find the value of the self energy $\Sigma_{\alpha_A \alpha_B}(\omega)$ is around the order of the boundary size l_{AB} . We therefore find the Green's function given by

$$G_{\alpha_A \alpha_B}(\omega) = \frac{1}{\omega - E_{\alpha_A}^A - E_{\alpha_B}^B - E^{(d)}(E_{\alpha_A}^A, E_{\alpha_B}^B) - \Sigma_{\alpha_A \alpha_B}(\omega)}. \quad (26)$$

On the other hand, it is known that the spectral weight is related to the eigenstates of Hamiltonian H by

$$A_{\alpha_A \alpha_B}(\omega) = 2\text{Im}G_{\alpha_A \alpha_B}(\omega) = 2\pi \sum_{\alpha} |\langle \alpha | \alpha_A, A; \alpha_B, B \rangle|^2 \delta(\omega - E_{\alpha}) = 2\pi \sum_{\alpha} |u_{\alpha, \alpha_A, \alpha_B}|^2 \delta(\omega - E_{\alpha}). \quad (27)$$

Therefore, in the large L_A, L_B limit, we approximately have (under the statistical average of h^{off}):

$$\begin{aligned} u_{\alpha, \alpha_A, \alpha_B} u_{\alpha, \alpha'_A, \alpha'_B}^* &\approx \frac{\delta_{\alpha_A, \alpha'_A} \delta_{\alpha_B, \alpha'_B}}{\pi N \Omega(E_{\alpha})} \text{Im}G_{\alpha_A \alpha_B}(E_{\alpha}) \\ &= \frac{\delta_{\alpha_A, \alpha'_A} \delta_{\alpha_B, \alpha'_B}}{\pi N \Omega(E_{\alpha})} \frac{|\Sigma_{\alpha_A \alpha_B}(E_{\alpha})|}{[E_{\alpha} - E_{\alpha_A}^A - E_{\alpha_B}^B - E^{(d)}(E_{\alpha_A}^A, E_{\alpha_B}^B)]^2 + |\Sigma_{\alpha_A \alpha_B}(E_{\alpha})|^2} \\ &\approx \frac{\delta_{\alpha_A, \alpha'_A} \delta_{\alpha_B, \alpha'_B}}{N \Omega(E_{\alpha})} \delta(E_{\alpha} - E_{\alpha_A}^A - E_{\alpha_B}^B - E^{(d)}(E_{\alpha_A}^A, E_{\alpha_B}^B)), \end{aligned} \quad (28)$$

where

$$\Omega(E) = \frac{1}{N} \sum_{\alpha} \delta(E - E_{\alpha}) \quad (29)$$

is the density of states of the entire system. Note that the energy width of the delta function in Eq. (28) is $|\Sigma_{\alpha_A \alpha_B}(E_{\alpha})|$, which is of order l_{AB} . It also has a dependence on E_{α} , $E_{\alpha_A}^A$ and $E_{\alpha_B}^B$ (see Eq. (24)). In comparison, the ranges of $E_{\alpha_A}^A$ and $E_{\alpha_B}^B$ are proportional to L_A and L_B . Therefore, the delta function approximation is legitimate when the subregion sizes L_A and L_B are large, in which case $l_{AB} \ll L_A$ and $l_{AB} \ll L_B$. The diagonal part $E^{(d)}$ of the boundary term yields an order l_{AB} contribution to the center position of the delta function.

If we take the approximation for $E^{(d)}(E_{\alpha_A}^A, E_{\alpha_B}^B)$ in Eq. (17), and assume $l_{AB} \ll L_A, L_B$, we find

$$\begin{aligned} \langle \alpha_A, A | \rho_A(\alpha) | \alpha'_A, A \rangle &= \sum_{\alpha_B} u_{\alpha, \alpha_A, \alpha_B} u_{\alpha, \alpha'_A, \alpha_B}^* \\ &\approx \int dE^B \frac{\delta_{\alpha_A, \alpha'_A} N_B}{N \Omega(E_{\alpha})} \Omega_B(E_B) \delta\left(E - E_{\alpha_A}^A - E^B - \frac{l_{AB}}{\epsilon_0^{AB}} \left(\frac{E_{\alpha_A}^A}{L_A} - \epsilon_0^A\right) \left(\frac{E^B}{L_B} - \epsilon_0^B\right)\right) \\ &= \delta_{\alpha_A, \alpha'_A} \frac{\Omega_B(a_A(E_{\alpha}, E_{\alpha_A}^A))}{N_A \Omega(E_{\alpha})}, \end{aligned} \quad (30)$$

where the function

$$a_A(E_{\alpha}, E_{\alpha_A}^A) = \frac{E - E_{\alpha_A}^A + \frac{\epsilon_0^B}{\epsilon_0^{AB}} \frac{l_{AB}}{L_A} (E_{\alpha_A}^A - L_A \epsilon_0^A)}{1 + \frac{l_{AB}}{\epsilon_0^{AB} L_B} \left(\frac{E_{\alpha_A}^A}{L_A} - \epsilon_0^A\right)}. \quad (31)$$

When $l_{AB} \ll L_A \ll L_B$, to the linear order of $E_{\alpha_A}^A - L_A \epsilon_0^A$ (note that the average value of $E_{\alpha_A}^A$ is $E_{av}^A = L_A \epsilon_0^A$), we approximately have

$$H_E^A(\alpha) = -\log \rho_A(\alpha) \approx \sum_{\alpha_A} \left(\beta_A^{(0)}(\alpha) + \beta_A^{(1)}(\alpha) E_{\alpha_A}^A \right) |\alpha_A, A\rangle \langle \alpha_A, A| = \beta_A^{(0)}(\alpha) I_A + \beta_A^{(1)}(\alpha) (H_A - E_{av}^A), \quad (32)$$

where

$$\beta_A^{(0)}(\alpha) = \log \left[\frac{N_A \Omega(E_\alpha)}{\Omega_B(E_\alpha - L_A \epsilon_0^A)} \right], \quad \beta_A^{(1)}(\alpha) = \left(1 + \frac{E_\alpha - L_A \epsilon_0^A - L_B \epsilon_0^B}{\epsilon_0^{AB}} \frac{l_{AB}}{L_A L_B} \right) \frac{d \log \Omega_B(E)}{dE} \Big|_{E=E_\alpha - L_A \epsilon_0^A}. \quad (33)$$

Note that by definition in Eq. (18) and the fact that $\text{tr}(H_{AB}) = 0$, we have $L_A \epsilon_0^A + L_B \epsilon_0^B = \text{tr}(H)/N = E_{av}$ is the average value of the energy E_α of the entire system. Also, note that $L_A \epsilon_0^A = E_{av}^A$ is the mean value of subregion energy $E_{\alpha_A}^A$, so we can rewrite the coefficients as

$$\beta_A^{(0)}(\alpha) = \log \left[\frac{N_A \Omega(E_\alpha)}{\Omega_B(E_\alpha - E_{av}^A)} \right], \quad \beta_A^{(1)}(\alpha) = \left(1 + \frac{E_\alpha - E_{av}}{\epsilon_0^{AB}} \frac{l_{AB}}{L_A L_B} \right) \frac{d \log \Omega_B(E)}{dE} \Big|_{E=E_\alpha - E_{av}^A}. \quad (34)$$

If we ignore all the terms to the linear order of $\frac{l_{AB}}{L_A}$, $\frac{l_{AB}}{L_B}$ and higher, we will have

$$\beta_A^{(0)}(\alpha) = \log \left[\frac{N_A \Omega(E_\alpha)}{\Omega_B(E_\alpha - E_{av}^A)} \right], \quad \beta_A^{(1)}(\alpha) \approx \frac{d \log \Omega_B(E)}{dE} \Big|_{E=E_\alpha - E_{av}^A}. \quad (35)$$

C. The case when the Hamiltonian is extremely nonlocal

For completeness, we also discuss the case when the Hamiltonian H is extremely nonlocal, in which case most terms are coupling subregions A and B and belong to H_{AB} , so we expect $\|H_{AB}\| \gg \|H_0\|$ in Eq. (13). We can then approximately regard $H_0 = 0$, and treat H_{AB} as a fully random matrix (as a nonlocal chaotic system resembles a zero dimensional chaotic system). Accordingly, if we assume the random matrix H_{AB} satisfies

$$\langle (H_{AB})_{\alpha'_A \alpha'_B; \alpha_A \alpha_B} (H_{AB})_{\alpha_A \alpha_B; \alpha'_A \alpha'_B} \rangle = \frac{\lambda^2}{N}, \quad (36)$$

the SD equation gives the Green's function and spectral weight

$$G_{\alpha_A \alpha_B}(\omega) = \frac{\omega - \sqrt{\omega^2 - 4\lambda^2}}{2\lambda^2}, \quad A_{\alpha_A \alpha_B}(\omega) = \Theta(4\lambda^2 - \omega^2) \frac{\sqrt{4\lambda^2 - \omega^2}}{\lambda^2}, \quad (37)$$

where $\Theta(x)$ is the Heaviside step function. Note that $A_{\alpha_A \alpha_B}(\omega)$ has no dependence on the basis indices α_A, α_B . Therefore, the eigenstate wavefunction components have no obvious α_A, α_B dependence, and we expect a uniform correlation

$$u_{\alpha, \alpha_A, \alpha_B} u_{\alpha, \alpha'_A, \alpha'_B}^* \approx \frac{\delta_{\alpha_A, \alpha'_A} \delta_{\alpha_B, \alpha'_B}}{N}. \quad (38)$$

S2. ENTANGLEMENT HAMILTONIAN OF SYSTEMS WITH MULTIPLE CONSERVED QUANTITIES

In this section, we consider the case when there are multiple local or quasilocal conserved quantities. We assume the system in the entire region has linearly independent conserved quantities $Q^{(n)}$ ($n \geq 1$) as shown in main text Eqs. (6) and (7), namely,

$$Q^{(n)}|\alpha\rangle = q_\alpha^{(n)}|\alpha\rangle, \quad [Q^{(n)}, Q^{(m)}] = 0, \quad Q^{(n)} = Q_A^{(n)} \otimes I_B + I_A \otimes Q_B^{(n)} + Q_{AB}^{(n)}, \quad (39)$$

where $Q_A^{(n)}$ ($Q_B^{(n)}$) has supports within subregion A (B), and $Q_{AB}^{(n)}$ contains all the terms with supports across the two subregions, as we defined below the main text Eq. (7). We assume $Q^{(0)} = I$ is the trivial identity operator. The full Hamiltonian H is given by a certain combination of $Q^{(n)}$ ($n \geq 0$). Without loss of generality, we assume different $Q^{(n)}$ ($n \geq 0$) are orthogonal, namely, their Frobenius inner product $(Q^{(n)}, Q^{(m)}) = \text{tr}(Q^{(n)} Q^{(m)}) \propto \delta_{mn}$. In particular, this indicates that $\text{tr}(Q^{(n)}) = \text{tr}(Q^{(n)} Q^{(0)}) = 0$ if $n \geq 1$, so $Q^{(n)}$ ($n \geq 1$) only contains traceless terms. Accordingly, the mean value of $q_\alpha^{(n)}$ for $n \geq 1$ is zero.

We now discuss the effect of conserved quantities $Q^{(n)}$ in a system on the statistical average value of the wavefunction correlation $u_{\alpha, \alpha_A, \alpha_B} u_{\alpha, \alpha'_A, \alpha'_B}^*$ under the subregion eigenstate direct product basis $|\alpha_A, A\rangle \otimes |\alpha_B, B\rangle$.

— *Case (i)*. If the conserved quantity $Q^{(n)}$ ($n \geq 1$) is local or quasilocal (and is extensive), in the large system size limit $l_{AB} \ll L_A, L_B$, we expect

$$\frac{||[H_A, Q_A^{(n)}]||}{||H_A|| ||Q_A^{(n)}||} \propto \frac{l_{AB}}{L_A} \rightarrow 0, \quad \frac{||[H_B, Q_B^{(n)}]||}{||H_B|| ||Q_B^{(n)}||} \propto \frac{l_{AB}}{L_B} \rightarrow 0. \quad (40)$$

Thus, one can approximately regard $[H_A, Q_A^{(n)}] = 0$ and $[H_B, Q_B^{(n)}] = 0$ as true, namely, $Q_A^{(n)}$ and $Q_B^{(n)}$ are approximate conserved quantities in subregions A and B , respectively. We therefore assume the subregion energy eigenstates approximately satisfy

$$Q_A^{(n)} |\alpha_A, A\rangle = q_{A, \alpha_A}^{(n)} |\alpha_A, A\rangle, \quad Q_B^{(n)} |\alpha_B, B\rangle = q_{B, \alpha_B}^{(n)} |\alpha_B, B\rangle. \quad (41)$$

Since $Q^{(n)}$ ($n \geq 1$) is traceless, $Q_A^{(n)}$, $Q_B^{(n)}$ and $Q_{AB}^{(n)}$ should also be traceless, and thus the mean values of $q_{A, \alpha_A}^{(n)}$ and $q_{B, \alpha_B}^{(n)}$ should vanish.

We further assume that the boundary coupling term $Q_{AB}^{(n)}$ exhibit certain randomness in its off diagonal elements in the subregion eigenstate direct product basis $|\alpha_A, A\rangle \otimes |\alpha_B, B\rangle$, similar to H_{AB} in Eq. (16). Then, in analogy to Eq. (28), under the random average of the off diagonal part of $Q_{AB}^{(n)}$, we expect the wavefunction correlation to satisfy $u_{\alpha, \alpha_A, \alpha_B} u_{\alpha, \alpha'_A, \alpha'_B}^* \propto \delta_{\alpha_A, \alpha'_A} \delta_{\alpha_B, \alpha'_B}$, and to be large only if $|q_\alpha^{(n)} - q_{A, \alpha_A}^{(n)} - q_{B, \alpha_B}^{(n)} - q_{\alpha_A, \alpha_B}^{(n, d)}|$ to be of order l_{AB} , where $q_{\alpha_A, \alpha_B}^{(n, d)}$ is the diagonal element of $Q_{AB}^{(n)}$ (which is of order l_{AB}). Since $q_\alpha^{(n)}$, $q_{A, \alpha_A}^{(n)}$ and $q_{B, \alpha_B}^{(n)}$ are of order L , L_A and L_B , respectively, in the $l_{AB} \ll L_A, L_B$ limit, we approximately have $u_{\alpha, \alpha_A, \alpha_B} u_{\alpha, \alpha'_A, \alpha'_B}^* \propto \delta_{\alpha_A, \alpha'_A} \delta_{\alpha_B, \alpha'_B} \delta(q_\alpha^{(n)} - q_{A, \alpha_A}^{(n)} - q_{B, \alpha_B}^{(n)} - q_{\alpha_A, \alpha_B}^{(n, d)})$. Note that $Q_{AB}^{(n)}$ is traceless, the average value of $q_{\alpha_A, \alpha_B}^{(n, d)}$ over all states is zero.

— *Case (ii)*. If the conserved quantity $Q^{(n)}$ is nonlocal, in the large system size limit we will have $Q_{AB}^{(n)}$ comparable or even larger than $Q_A^{(n)} \otimes I_B$ and $I_A \otimes Q_B^{(n)}$. Therefore, $Q_A^{(n)}$ or $Q_B^{(n)}$ will not be approximate subregion conserved quantities. In this case, we expect the entire $Q^{(n)}$ matrix to be sufficiently random (due to the $Q_{AB}^{(n)}$ term) in the subregion eigenstate direct product basis $|\alpha_A, A\rangle \otimes |\alpha_B, B\rangle$, and won't contribute to the shape of the statistical average of the wavefunction correlation $u_{\alpha, \alpha_A, \alpha_B} u_{\alpha, \alpha'_A, \alpha'_B}^*$.

With the arguments in the two above cases, we expect the eigenstate wavefunction correlation in the large system size limit to be approximately

$$u_{\alpha, \alpha_A, \alpha_B} u_{\alpha, \alpha'_A, \alpha'_B}^* = \frac{1}{N} \delta_{\alpha_A, \alpha'_A} \delta_{\alpha_B, \alpha'_B} \prod_{n \in \text{Loc}} \frac{1}{\Omega^{(n)}(q_\alpha^{(n)})} \delta(q_\alpha^{(n)} - q_{A, \alpha_A}^{(n)} - q_{B, \alpha_B}^{(n)} - q_{\alpha_A, \alpha_B}^{(n, d)}), \quad (42)$$

where

$$\Omega^{(n)}(q) = \frac{1}{N} \sum_{\alpha} \delta(q - q_\alpha^{(n)}) \quad (43)$$

denotes the normalized density of states of the operator $Q^{(n)}$, and $n \in \text{Loc}$ runs over all the local or quasilocal nontrivial conserved quantities $Q^{(n)}$ with $n \geq 1$. Note that when there is only one local or quasilocal conserved quantity, which has to be the Hamiltonian H , Eq. (42) reduces to Eq. (28).

This yields a reduced density matrix in subregion A (where we used the fact that the mean value of $q_{\alpha_A, \alpha_B}^{(n, d)}$ is zero for $n \geq 1$)

$$\begin{aligned} \langle \alpha_A, A | \rho_A(\alpha) | \alpha'_A, A \rangle &= \sum_{\alpha_B} u_{\alpha, \alpha_A, \alpha_B} u_{\alpha, \alpha'_A, \alpha_B}^* \approx \frac{\delta_{\alpha_A, \alpha'_A} N_B}{N} \int dE_B \frac{\Omega_B^{(n)}(q_B^{(n)})}{\Omega^{(n)}(q_\alpha^{(n)})} \delta(q_\alpha^{(n)} - q_{A, \alpha_A}^{(n)} - q_{B, \alpha_B}^{(n)}) dq_B^{(n)} \\ &= \frac{\delta_{\alpha_A, \alpha'_A}}{N_A} \prod_{n \in \text{Loc}} \frac{\Omega_B^{(n)}(q_\alpha^{(n)}(q_\alpha^{(n)}, q_{A, \alpha_A}^{(n)}))}{\Omega^{(n)}(q_\alpha^{(n)})}, \end{aligned} \quad (44)$$

where

$$\Omega_B^{(n)}(q_B^{(n)}) = \frac{1}{N_B} \sum_{\alpha_B} \delta(q - q_{B, \alpha_B}^{(n)}) \quad (45)$$

is the normalized density of states of the subregion conserved quantity $Q_B^{(n)}$, and similar to Eq. (31), one expects the function

$$a_A^{(n)}(q_\alpha^{(n)}, q_{A,\alpha_A}^{(n)}) \approx q_\alpha^{(n)} - q_{A,\alpha_A}^{(n)} \quad (46)$$

in the limit $l_{AB} \ll L_A, L_B$.

If further we are in the limit $l_{AB} \ll L_A \ll L_B$, we can expand over $q_{A,\alpha_A}^{(n)}$ ($n \geq 1$) to the first order, which yields an approximate entanglement Hamiltonian of subregion A given by

$$H_E^A(\alpha) \approx \beta_A^{(0)}(\alpha) I_A + \sum_{n \in \text{Loc}} \beta_A^{(n)}(\alpha) Q_A^{(n)}. \quad (47)$$

Note that the set $n \in \text{Loc}$ does not include $n = 0$, which correspond to the trivial conserved quantity of the identity matrix. Similar to Eq. (34), and note that the mean values of $q_\alpha^{(n)}$ and $q_{A,\alpha_A}^{(n)}$ are zero, we find the coefficients are approximately given by

$$\beta_A^{(n)}(\alpha) = b_\alpha^{(n)} \frac{d \log \Omega_B^{(n)}(q)}{dq} \Big|_{q=q_\alpha^{(n)}}, \quad (n \in \text{Loc}), \quad \beta_A^{(0)}(\alpha) = \log N_A + \sum_{n \geq 1} \log \frac{\Omega_B^{(n)}(q_\alpha^{(n)})}{\Omega_B^{(n)}(q_\alpha^{(n)})}, \quad (48)$$

where $b_\alpha^{(n)} = 1 + \mathcal{O}\left(\frac{q_\alpha^{(n)} l_{AB}}{L_A L_B}\right)$ is a function which tends to 1 in the limit $l_{AB} \ll L_A, L_B$.

S3. DIAGONALIZATION OF THE EHSM

When the entanglement Hamiltonians $H_E^A(\alpha)$ in subregion A of an ensemble of the full region eigenstates $\alpha \in \Xi$ are known, all of which have the form of Eq. (47), we can solve for the conserved quantities and their weights in the entanglement Hamiltonians.

To do this, we can regard each entanglement Hamiltonian $H_E^A(\alpha)$ (written down in a certain Hilbert space basis $|j\rangle$) as a vector in the linear space of $N_A \times N_A$ matrices. More explicitly, we can define a matrix basis $|\zeta_{ij}\rangle$ ($1 \leq i, j \leq N_A$) which represents an $N_A \times N_A$ matrix with matrix elements $\delta_{ii'} \delta_{jj'}$ in row i' and column j' . Here half parenthesis instead of ket is used to denote the matrix basis, to avoid confusion with the quantum state basis. We can then rewrite the entanglement Hamiltonian $H_E^A(\alpha)$ as a vector $|H_E^A(\alpha)\rangle = \sum_{i,j} H_{E,ij}^A(\alpha) |\zeta_{ij}\rangle$, where $H_{E,ij}^A$ represent the matrix elements of H_E^A in row i and column j . Thus, the inner product between two matrices P and Q are exactly the Frobenius inner product, namely, $(Q|P) = \text{tr}(Q^\dagger P)$.

As given in the main text Eq. (9), we then define the entanglement Hamiltonian superdensity matrix (EHSM) for the set of entanglement Hamiltonians:

$$R_A = \sum_{\alpha \in \Xi} \frac{w_\alpha}{N_A} |H_E^A(\alpha)\rangle \langle H_E^A(\alpha)| = \sum_{\alpha \in \Xi} \sum_{ij i' j'} \frac{w_\alpha}{N_A} H_{E,ij}^A(\alpha) H_{E,i'j'}^{A*}(\alpha) |\zeta_{ij}\rangle \langle \zeta_{i'j'}|, \quad (49)$$

where for generality we assume one is free to set a weight $w_\alpha > 0$ for each eigenstate $|\alpha\rangle$ in the ensemble Ξ , and $\sum_{\alpha \in \Xi} w_\alpha = 1$. Note that the EHSM R_A is a size $N_A^2 \times N_A^2$ matrix. Assume the EHSM can be diagonalized into into

$$R_A = \sum_{n \geq 0} p_{A,n} |\bar{Q}_A^{(n)}\rangle \langle \bar{Q}_A^{(n)}|, \quad (50)$$

where the eigenvectors $|\bar{Q}_A^{(n)}\rangle$ are orthonormal, namely, they satisfy $\langle \bar{Q}_A^{(m)} | \bar{Q}_A^{(n)} \rangle = \text{tr}(\bar{Q}_A^{(m)\dagger} \bar{Q}_A^{(n)}) = \delta_{mn}$. We note that the matrices $\bar{Q}_A^{(n)}$ as normalized eigenvectors here are not necessarily equal to $Q_A^{(n)}$ in Eq. (47), although we expect that they span the same linear space of size $N_A \times N_A$ matrices. Generically, a physical local or quasilocal conserved quantity would have a Frobenius norm $\|Q_A^{(n)}\| \propto \sqrt{N_A L_A}$, therefore, we expect the physical conserved quantities $Q_A^{(n)} \sim \sqrt{N_A L_A} \bar{Q}_A^{(n)}$.

Generically, the EHSM is a big matrix of size $N_A^2 \times N_A^2$. When the number of eigenstates N_Ξ in the ensemble Ξ is much smaller than N_A^2 , an efficient way of diagonalizing R_A is to diagonalize the following $N_\Xi \times N_\Xi$ entanglement correlation matrix S_A with matrix elements

$$S_{A,\alpha\beta} = \frac{\sqrt{w_\alpha w_\beta}}{N_A} (H_E^A(\alpha) | H_E^A(\beta)) , \quad (51)$$

where $\alpha, \beta \in \Xi$. We now prove that the eigenvalues of the correlation matrix S_A are the same as the nonzero eigenvalues of the EHSM R_A , and their eigenvectors have a simple relation. Assume the n -th eigenvector of S_A is v_n^A ($n \geq 0$), which satisfies

$$\sum_{\beta} S_{A,\alpha\beta} v_{n,\beta}^A = p_{A,n} v_{n,\alpha}^A, \quad v_m^{A\dagger} v_n = \sum_{\alpha} v_{m,\alpha}^{A*} v_{n,\alpha}^A = \delta_{mn}, \quad (52)$$

where we assume the eigenvalues $p_{A,n}$ are ranked in a descending order. We can then define a vector in the matrix space $|\bar{Q}_A^{(n)}\rangle = \frac{1}{\sqrt{N_A p_{A,n}}} \sum_{\beta} \sqrt{w_{\beta}} v_{n,\beta}^A |H_E^A(\beta)\rangle$, which has been normalized, namely, $(\bar{Q}_A^{(n)} | \bar{Q}_A^{(n)}) = 1$. One can then verify that $|\bar{Q}_A^{(n)}\rangle$ is an eigenvector of the EHSM R_A with eigenvalue $p_{A,n}$:

$$\begin{aligned} R_A |\bar{Q}_A^{(n)}\rangle &= \frac{1}{\sqrt{N_A p_{A,n}}} \sum_{\alpha\beta} w_{\alpha} \sqrt{w_{\beta}} v_{n,\beta}^A |H_E^A(\alpha)\rangle (H_E^A(\alpha) | H_E^A(\beta)\rangle) = \frac{1}{\sqrt{N_A p_{A,n}}} \sum_{\alpha\beta} \sqrt{w_{\alpha}} |H_E^A(\alpha)\rangle S_{A,\alpha\beta} v_{n,\beta}^A \\ &= \frac{1}{\sqrt{N_A p_{A,n}}} \sum_{\alpha} p_{A,n} \sqrt{w_{\alpha}} v_{n,\alpha}^A |H_E^A(\alpha)\rangle = p_{A,n} |\bar{Q}_A^{(n)}\rangle, \end{aligned} \quad (53)$$

where we have used Eq. (52). Note that the rank of matrices R_A and S_A are both equal to N_{Ξ} , so they have equal number of nonzero eigenvalues. Therefore, we conclude that the eigenvalues $p_{A,n}$ of matrix S_A are exactly equal to all the nonzero eigenvalues of R_A , and the relation between their corresponding eigenvectors are given by Eq. (53). Numerically, it is easier to diagonalize S_A if the number of eigenstates $N_{\Xi} < N_A^2$, which is equivalent to the diagonalization of R_A .

S4. THE EHSM OF FREE FERMIONS

In this section, we give the details on the diagonalization of the EHSM of the free fermion model given in main text Eq. (11), namely,

$$H = -t \sum_{\langle ij \rangle} (c_{\mathbf{r}_i}^{\dagger} c_{\mathbf{r}_j} + h.c.) + \sum_j \mu_j c_{\mathbf{r}_j}^{\dagger} c_{\mathbf{r}_j}, \quad (54)$$

which has one fermion degree of freedom per site i , where t is the nearest neighbor hopping, and μ_i is a random potential distributed within the interval $[-W, W]$. We assume the l -th single-particle eigenstate wavefunctions of the full region are $\phi_{l,i}$ ($1 \leq l \leq L$), with the single-particle energy being ϵ_l . Accordingly, the many-body eigenstates are generically given by

$$|\alpha\rangle = \prod_{l=1}^L (f_l^{\dagger})^{\eta_{\alpha,l}} |0\rangle, \quad f_l^{\dagger} = \sum_i \phi_{l,i} c_{\mathbf{r}_i}^{\dagger}, \quad (55)$$

where f_l^{\dagger} are the single-particle eigenstate fermion creation operators, $\eta_{\alpha,l} = 0$ or 1 is the occupation number of single-particle state l , and $|0\rangle$ is the particle number vacuum with zero fermions. According to Ref. [37], the entanglement Hamiltonian of the free fermion state $|\alpha\rangle$ in subregion A is given by

$$H_E^A(\alpha) = \gamma_A(\alpha) I_A + \sum_{i,j \in A} \kappa_{A,ij}(\alpha) c_{\mathbf{r}_i}^{\dagger} c_{\mathbf{r}_j}, \quad (56)$$

where the matrix $\kappa_A(\alpha)$ and the number $\gamma_A(\alpha)$ are defined by

$$\kappa_A(\alpha) = \log(\mathcal{C}_A(\alpha)^{-1} - I_A), \quad \gamma(\alpha) = -\text{tr} \log(I_A - \mathcal{C}_A(\alpha)), \quad (57)$$

in terms of the $L_A \times L_A$ 2-particle correlation matrix $\mathcal{C}_A(\alpha)$ with matrix elements

$$\mathcal{C}_{A,ij}(\alpha) = \langle \alpha | c_{\mathbf{r}_i}^{\dagger} c_{\mathbf{r}_j} | \alpha \rangle = \sum_{l=1}^L \eta_{\alpha,l} \phi_{l,i} \phi_{l,j}^*, \quad (i, j \in A) \quad (58)$$

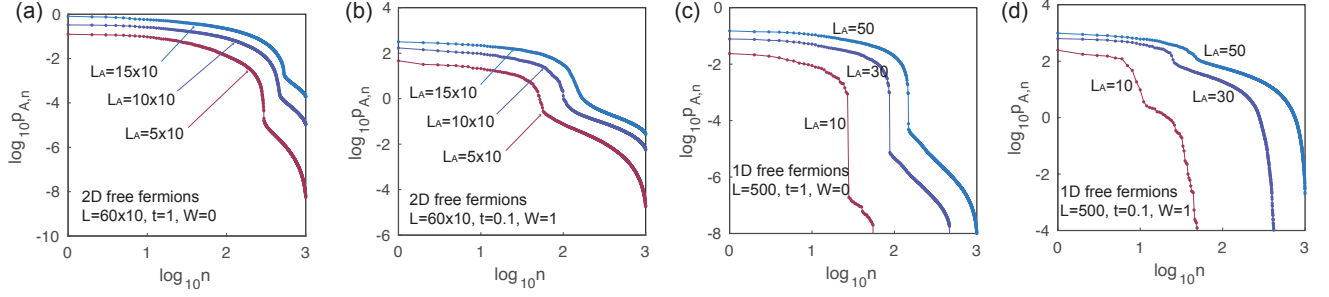


FIG. 5. The log-log plot ($\log_{10} p_{A,n}$ vs. $\log_{10} n$) of the EHS eigenvalues $p_{A,n}$ for free fermion models in 2D ((a)-(b)) and in 1D ((c)-(d)), which are calculated for randomly chosen 1000 many-body eigenstates. The Hamiltonian is given by Eq. (54), and the parameters are labeled in the panels. For 2D ((a)-(b)), the system size is given by $L = L_x L_y$, with $L_x = 60$ and $L_y = 10$ fixed, while the A subsystem size is $L_A = L_{Ax} L_y$ with $L_{Ax} = 5, 10, 15$ examined. For 1D ((c)-(d)), the system size is $L = 500$, and the A subsystem sizes $L_A = 5, 10, 15$ are considered. In (a) and (c) when the single-particle states are delocalized, $p_{A,n}$ shows a sharp cutoff towards zero around $n = 3L_A$. In contrast, in (b) and (d) where the single-particle states are localized, $p_{A,n}$ shows a sharp cutoff towards zero around $n = L_A$.

Note that $H_E^A(\alpha)$ is a many-body Hamiltonian of size $N_A \times N_A$, while $\kappa_A(\alpha)$ and $\mathcal{C}_A(\alpha)$ are Hermitian matrices of size $L_A \times L_A$ (recall that L_A is the number of sites, and $N_A = 2^{L_A}$ in this model). In this case, the Frobenius inner products of entanglement Hamiltonians in Eq. (51) are given by

$$\begin{aligned}
 \langle H_E^A(\alpha) | H_E^A(\beta) \rangle &= \text{tr}(H_E^A(\alpha) H_E^A(\beta)) \\
 &= \sum_{ij i' j' \in A} (\kappa_A(\alpha))_{ij} (\kappa_A(\beta))_{i' j'} \text{tr}(c_i^\dagger c_j c_{i'}^\dagger c_{j'}) + \gamma(\alpha) \sum_{ij \in A} (\kappa_A(\beta))_{ij} \text{tr}(c_i^\dagger c_j) + \gamma(\beta) \sum_{ij \in A} (\kappa_A(\alpha))_{ij} \text{tr}(c_i^\dagger c_j) + \gamma(\alpha) \gamma(\beta) \text{tr} I_A \\
 &= \sum_{ij i' j' \in A} (\kappa_A(\alpha))_{ij} (\kappa_A(\beta))_{i' j'} \frac{N_A}{4} (\delta_{ij} \delta_{i' j'} + \delta_{i' j} \delta_{ij'}) + \gamma(\alpha) \sum_i \frac{N_A}{2} (\kappa_A(\beta))_{ii} + \gamma(\beta) \sum_i \frac{N_A}{2} (\kappa_A(\alpha))_{ii} + \gamma(\alpha) \gamma(\beta) N_A \\
 &= N_A \left\{ \frac{1}{4} \text{tr}[\kappa_A(\alpha) \kappa_A(\beta)] + \left(\frac{1}{2} \text{tr}[\kappa_A(\alpha)] + \gamma(\alpha) \right) \left(\frac{1}{2} \text{tr}[\kappa_A(\beta)] + \gamma(\beta) \right) \right\}.
 \end{aligned} \tag{59}$$

This greatly simplifies the calculation of the matrix S_A in Eq. (51), and thus the diagonalization of the EHS R_A of free fermions.

A. Numerical results

We numerically diagonalize the EHS of the free fermion Anderson model (54) in both 1D and 2D (the lattices of which are illustrated in the main text Fig. 1):

(i) In the 2D case, the system is in a lattice with $L_x = 60$ and $L_y = 10$ sites in the x and y directions, with periodic boundary condition in both directions. We set the lattice constant in both directions to be 1. The full 2D number of sites is thus $L = L_x L_y = 600$. The 2D subregion A is defined to be the region of sites within x coordinate $1 \leq x_j \leq L_{A,x}$ as shown in the main text Fig. 1a (here (x_j, y_j) is the 2D coordinate of site j), which has number of sites $L_A = L_{A,x} L_y$.

(ii) In the 1D case, we set the number of sites in the system to be $L = 500$, with a periodic boundary condition. The 1D subregion A is chosen to be the region of sites within the x coordinate $1 \leq x_j \leq L_A$.

In both cases, we calculate and diagonalize the EHS for an ensemble Ξ of randomly chosen $N_\Xi = 1000$ eigenstates of the full system, and each of the eigenstates has an equal weight $w_\alpha = 1/N_\Xi$ in the EHS in Eq. (49). We note that if the 2-particle correlation matrix $\mathcal{C}(\alpha)$ in Eq. (58) has eigenvalues reaching 0 or 1, the entanglement Hamiltonian coefficients in Eq. (57) will encounter divergence. To avoid such numerical divergences, we relax the 0 and 1 eigenvalues of $\mathcal{C}(\alpha)$, if any, into δ and $1 - \delta$, respectively, with δ being a sufficiently small positive number. In practice, we set $\delta = 10^{-16}$. We note that $\mathcal{C}(\alpha)$ has almost 0 or 1 eigenvalues only when the single-particle eigenstates of the system are localized. We also verified that the numerical EHS eigenvalues are insensitive to the cutoff δ .

The leading eigenvalues $p_{A,n}$ of the EHS for several different parameters in 2D and 1D are shown in the main text Fig. 2 in a descending order (the values of $p_{A,n}/L_A$ are plotted). In 2D, we show the results for A subregion

sizes $L_{Ax} = 5, 10, 15$ (corresponding to $L_A = 50, 100, 150$), while in 1D, we show the results for A subregion sizes $L_A = 10, 30, 50$. The logarithm $\log_{10} p_{A,n}$ of the eigenvalues $p_{A,n}$ with respect to $\log_{10} n$ are shown in Fig. 5. We now discuss the results for extended fermions and localized fermions, respectively.

1. Extended fermions

Fig. 5 (a) and (c) shows the results for $t = 1$ and $W = 0$, in 2D and 1D, respectively. In this case, the single-particle states of the entire system are delocalized plane waves. As shown in Fig. 5 (a) and (c), in this case with extended single-particle fermion eigenstates, we find the eigenvalues $p_{A,n}$ decays to 0 around $n = 3L_A$ (which corresponds to the sharp drop in the log-log plot in Fig. 5). Indeed, if we examine the subregion A which has open boundary condition in the x direction (and periodic boundary condition in the y direction), we can approximately find $3L_A$ conserved quantities, as we will explain now.

Assume the x coordinate of subregion A ranges from 1 to $L_{A,x}$. The total number of sites in subregion A is $L_A = L_{A,x}L_y$, where $L_y > 1$ ($L_y = 1$) if the system is in 2D (1D). If we take open boundary condition in the x direction, the subregion A eigenstates will be standing waves in the x direction, the creation operators of which are given by

$$\frac{c_{A,k_x,k_y}^\dagger - c_{A,-k_x,k_y}^\dagger}{\sqrt{2}}, \quad (60)$$

where $c_{A,k_x,k_y}^\dagger = \frac{1}{\sqrt{L_A}} \sum_{j \in A} e^{-ik_x x_j - ik_y y_j} c_{x_i, y_i}^\dagger$ is the momentum \mathbf{k} eigenstate, $k_x = \frac{\pi m_x}{L_{A,x}+1}$, $k_y = \frac{2\pi m_y}{L_y}$, and $m_x, m_y \in \mathbb{Z}$. Accordingly, the subregion A Hamiltonian H_A can be diagonalized into

$$\begin{aligned} H_A &= \sum_{k_x > 0} \sum_{k_y} \epsilon(\mathbf{k}) \left(\frac{c_{A,k_x,k_y}^\dagger - c_{A,-k_x,k_y}^\dagger}{\sqrt{2}} \right) \left(\frac{c_{A,k_x,k_y} - c_{A,-k_x,k_y}}{\sqrt{2}} \right) \\ &= \frac{1}{2} \sum_{k_x > 0} \sum_{k_y} \epsilon(\mathbf{k}) \left[\left(c_{A,k_x,k_y}^\dagger c_{A,k_x,k_y} + c_{A,-k_x,k_y}^\dagger c_{A,-k_x,k_y} \right) - \left(c_{A,-k_x,k_y}^\dagger c_{A,k_x,k_y} + c_{A,k_x,k_y}^\dagger c_{A,-k_x,k_y} \right) \right], \end{aligned} \quad (61)$$

where $\epsilon(\mathbf{k}) = -2t(\cos k_x + \cos k_y)$. In particular, this gives the following conserved quantities:

$$\tilde{T}_{k_x,k_y}^A = c_{A,k_x,k_y}^\dagger c_{A,k_x,k_y} + c_{A,-k_x,k_y}^\dagger c_{A,-k_x,k_y}, \quad \tilde{P}_{k_x,k_y}^A = c_{A,-k_x,k_y}^\dagger c_{A,k_x,k_y} + c_{A,k_x,k_y}^\dagger c_{A,-k_x,k_y}, \quad (62)$$

which one can easily verify. One can linearly recombine these conserved quantities into the following forms in the real space:

$$\begin{aligned} T_{x,y}^A &= \sum_{k_x,k_y} e^{ik_x x + ik_y y} \tilde{T}_{k_x,k_y}^A \approx \sum_i (c_{x_i+x, y_i+y}^\dagger c_{x_i, y_i} + c_{x_i, y_i+y}^\dagger c_{x_i+x, y_i}), \\ P_{x,y}^A &= \frac{1}{2} \sum_{k_x,k_y} e^{-ik_x x + ik_y y} \tilde{P}_{k_x,k_y}^A \approx \sum_i c_{x-x_i, y_i+y}^\dagger c_{x_i, y_i}, \end{aligned} \quad (63)$$

where all the fermion operators $c_{\mathbf{r}}^\dagger$ and $c_{\mathbf{r}}$ are restricted within subregion A . Here y_j identified with $y_j + L_y$, and $x, y \in \mathbb{Z}$.

We now estimate how many such conserved quantities are there. Note that $1 \leq x_i \leq L_{A,x}$, while y_i is periodic with total length L_y . Therefore, for quantity $T_{x,y}^A$, we can take $0 \leq x \leq L_{A,x} - 1$, and $0 \leq y \leq L_y - 1$, which in total yields about $L_A = L_{A,x}L_y$ linearly independent quantities $T_{x,y}^A$. In contrast, for quantity $P_{x,y}^A$, the x coordinate can take values $2 \leq 2L_{A,x}$, while $0 \leq y \leq L_y - 1$. Therefore, there are in total $2L_A - 1$ linearly independent quantities $P_{x,y}^A$. Together with the trivial identity I_A in subregion A , we find there are in total around $3L_A$ conserved quantities in subregion A .

To verify that the $3L_A$ nonzero EHSM eigenvalues $p_{A,n}$ correspond to conserved quantities in Eq. (63), we investigate the numerically obtained EHSM eigen-operators $\bar{Q}^{(n)}$. From Eq. (56), we know that $\bar{Q}^{(n)}$ is of the fermion bilinear form

$$\bar{Q}^{(n)} = \gamma_A^{(n)} I_A + \sum_{i,j \in A} \kappa_{A,ij}^{(n)} c_{\mathbf{r}_i}^\dagger c_{\mathbf{r}_j}, \quad (64)$$

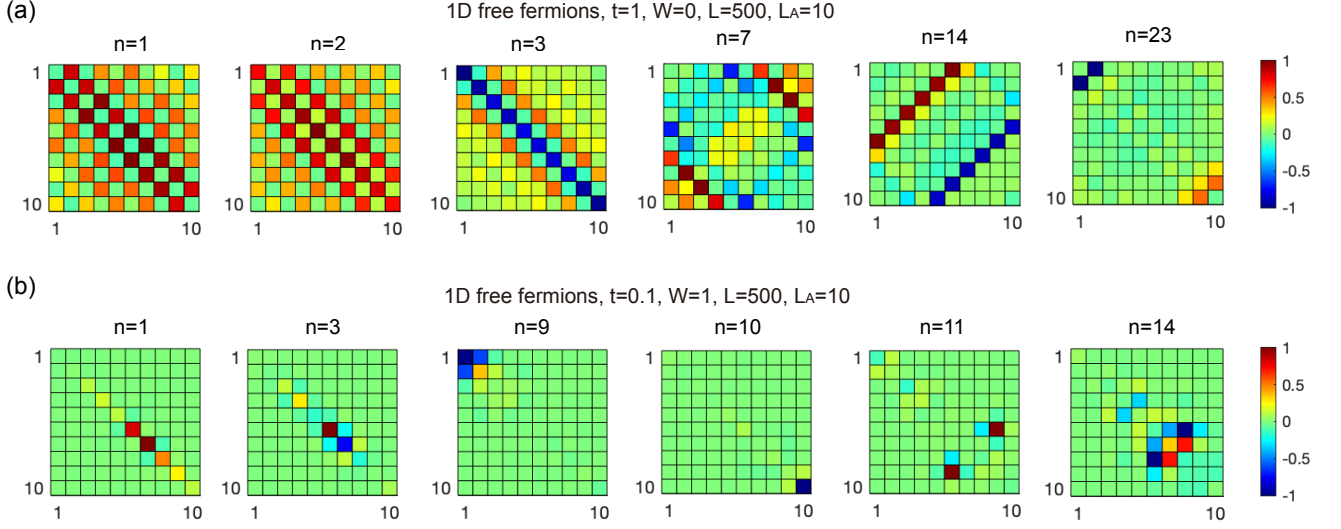


FIG. 6. The single-body matrices $\kappa_{A,ij}^{(n)}$ (as defined in Eq. (64)) of eigen-operators $\bar{Q}^{(n)}$ ($n \geq 1$) for 1D free fermions, where the entire system size is $L = 500$, and subregion size is $L_A = 10$. The x and y axes of each panel give the row and column indices of the matrices $\kappa_{A,ij}^{(n)}$, with i, j sorted along the lattice of subregion A from the left to the right. The colorbar values for each n are given in units of the maximal absolute value of matrix element $\kappa_{A,ij}^{(n)}$. (a) shows several examples for $t = 1$, $W = 0$ where the fermions are extended, while (b) shows a few examples for $t = 0.1$ and $W = 1$ where the fermions are localized.

where $\gamma_A^{(n)}$ is some constant, and $\kappa_{A,ij}^{(n)}$ is a matrix of size $L_A \times L_A$. In particular, we find that the $n = 0$ quantity is dominantly $\bar{Q}^{(0)} \propto I_A$, while for $n \geq 1$ we approximately have $\text{tr}(\bar{Q}^{(n)}) = 0$. In Fig. 6(a), we plot examples of the matrices $\kappa_{A,ij}^{(n)}$ ($n \geq 1$) for 1D free fermions with $t = 1$, $W = 0$, $L = 500$ and $L_A = 10$, where the x and y axis are the row and column indices of the matrices $\kappa_{A,ij}^{(n)}$. In particular, we find $\bar{Q}^{(n)}$ with $1 \leq n \leq L_A$ are approximately dominated by linear combinations of $T_{x,y}^A$ in Eq. (63). On the contrary, $\bar{Q}^{(n)}$ with $L_A < n \leq 3L_A$ are approximately dominated by linear combinations of $P_{x,y}^A$ in Eq. (63).

2. Localized fermions

In Fig. 5 (b) and (d) (see also the main text Fig. 1 (b) and (d)), we set the parameters to $t = 0.02$, $W = 1$ (in 2D) and $t = 0.1$, $W = 1$ (in 1D), respectively, in which case the single-particle states are strongly localized. In this case, we find the EHSM eigenvalues $p_{A,n}$ has a sharp cutoff around $n \approx L_A$: the eigenvalues $p_{A,n}$ with $n > L_A$ become vanishingly small compared to those with $n < L_A$. This can be seen more clearly in the main text Fig. 1 (b) and (d), and can also be seen by noting the kink around $n = L_A$ in Fig. 5 (b) and (d). This is because in the strongly localized limit, the single-particle eigenstates are almost localized on each site, namely, the l -th eigenstate fermion operators $f_l^\dagger \approx c_{\mathbf{r}_l}^\dagger$. As a result, one expect no long range entanglement, and the entanglement Hamiltonian in Eq. (56) almost only contains local fermion bilinear terms $c_{\mathbf{r}_l}^\dagger c_{\mathbf{r}_l}$ ($l \in A$). This would only yield L_A linearly independent eigen-operators $\bar{Q}_A^{(n)}$ with nonzero $p_{A,n}$ ($1 \leq n \leq L_A$), which are approximately the linear combinations of $2c_{\mathbf{r}_l}^\dagger c_{\mathbf{r}_l} - 1$ (so written that it is traceless). Besides, numerically we find $\bar{Q}^{(0)} \propto I_A$.

In Fig. 6(b), we have plotted the $\kappa_{A,ij}^{(n)}$ ($n \geq 1$) of the eigen-operators $\bar{Q}_A^{(n)}$ (defined in Eq. (64)) for 1D free fermions with $t = 1$, $W = 0$, $L = 500$ and $L_A = 10$. In the panels, the x and y axis are the row and column indices of the matrices $\kappa_{A,ij}^{(n)}$. As one can see, for $1 \leq n \leq L_A$, the eigen-operators $\bar{Q}_A^{(n)}$ are linear combinations of the occupation numbers of single-particle localized wavefunctions. Two examples with $n > L_A$ ($n = 11, 14$) are also shown in Fig. 6(b), which become less localized. Accordingly, their EHSM eigenvalues $p_{A,n}$ are vanishingly small compared to those of $n \leq L_A$.

S5. THE EHSM OF THE 1D XYZ MODEL IN A MAGNETIC FIELD

A. EHSM eigenvalues and entanglement entropies

We numerically study the EHSM of the 1D XYZ model, to which we can add either uniform or disordered magnetic fields. The model Hamiltonian is given by the main text Eq. (12), which we rewrite here:

$$H = \sum_{j=1}^L \left[J_x \sigma_{j,x} \sigma_{j+1,x} + J_y \sigma_{j,y} \sigma_{j+1,y} + J_z \sigma_{j,z} \sigma_{j+1,z} + (\mathbf{B} + \delta \mathbf{B}_j) \cdot \boldsymbol{\sigma}_j \right]. \quad (65)$$

Here $\sigma_{j,\nu}$ ($\nu = x, y, z$) are the Pauli matrices on site j . We have added both a uniform magnetic field B , and a random magnetic field $\delta \mathbf{B}_j$ with each component $\delta B_{j,\nu}$ independently randomly distributed in the interval $[-B_{R,\nu}, B_{R,\nu}]$ ($\nu = x, y, z$), in which \mathbf{B}_R is given. We perform the exact diagonalization of model (65) for a 1D lattice with $L = 14$ sites with periodic boundary condition. We then calculate the EHSM in subregion A of sizes L_A up to 7 (half of the system size).

In calculating the entanglement Hamiltonians, an entanglement Hamiltonian may have a diverging part if its corresponding reduced density matrix has an exactly zero eigenvalue. This may happen when the Hilbert space is fragmented into non-communicating subspaces. Such exactly zero eigenvalues usually does not occur in ρ_A if the system is delocalized, in which case such fragmented Hilbert subspace would involve both subregions A and B , thus is not a closed subspace within the Hilbert space of subregion A . However, if the system is localized, one may end up with almost or exact zero eigenvalues in ρ_A . In this case, we substitute the (almost) zero eigenvalues by a small number $\epsilon > 0$ to avoid divergence. We find the behaviors of the EHSM eigenvalues are rather insensitive to the small number cutoff ϵ . Here we take ϵ to 10^{-16} .

In the main text Fig. 3, we diagonalize the EHSM for the ensemble Ξ containing all the N eigenstates of the full region, with equal weights $w_\alpha = 1/N$ for all the eigenstates, and plot the EHSM eigenvalues $p_{A,n}$ with respect to n . The six panels of main text Fig. 3 correspond to six different representative sets of parameters (labeled at the top of the panels, see also below), and the sizes of subregion A we examined are $L_A = 4, 5, 6, 7$. Fig. 7 shows the log-log plot of the main text Fig. 3, namely, $\log_{10} p_{A,n}$ as a function of $\log_{10} n$.

Fig. 8 shows the subregion A (size $L_A = 7$) entanglement entropies

$$S_A(\alpha) = -\text{tr}(\rho_A(\alpha) \log \rho_A(\alpha)) \quad (66)$$

of all the eigenstates $|\alpha\rangle$ of the full region plotted versus the eigenstate energies E_α . The parameters of the 6 panels are the same as those in the main text Fig. 3 (and supplementary Fig. 7).

We first briefly describe the properties of the six sets of parameters in the six panels of the main text Fig. 3 (a)-(f) (as well as the supplementary Fig. 7 (a)-(f) and Fig. 8 (a)-(f)):

(a) $(J_x, J_y, J_z) = (1, 1, 1), \mathbf{B} = (0, 0, 10^{-10}), \mathbf{B}_R = (0, 0, 0)$. This is the isotropic case with equal spin couplings in all directions, known as the XXX model. In our calculations, we have added a very small magnetic field in the z direction to pin the energy eigenstates also into eigenstates of $\sum_j \sigma_{j,z}$, an obvious conserved quantity. The XXX model is known to be integrable (exactly solvable) by the Bethe ansatz, and a class of local and quasilocal conserved quantities have been derived in [7, 8].

(b) $(J_x, J_y, J_z) = (0.5, 0.5, 1), \mathbf{B} = (0, 0, 0), \mathbf{B}_R = (0, 0, 0)$. This set of parameters with $J_x = J_y$ gives the XXZ model, which is also integrable, and has a class of local conserved quantities [7].

(c) $(J_x, J_y, J_z) = (0.5, 0.8, 1), \mathbf{B} = (0, 0, 0), \mathbf{B}_R = (0, 0, 0)$. This is the generic XYZ model with three spin couplings unequal. The model is still integrable, and a class of local conserved quantities can be found [7].

(d) $(J_x, J_y, J_z) = (0.5, 0.8, 1), \mathbf{B} = (0, 0, 1), \mathbf{B}_R = (0, 0, 0)$. This is the generic XYZ model in a uniform magnetic field \mathbf{B} . It is proved that local conserved quantities do not exist for such a model [40]. However, this does not rule out the existence of quasilocal conserved quantities.

(e) $(J_x, J_y, J_z) = (0.5, 0.5, 1), \mathbf{B} = (0, 0, 0), \mathbf{B}_R = (0, 0, 5)$. This set of parameters give an XXZ model with a random magnetic field in the z direction. This model is expected to be in the MBL phase when the random magnetic field $B_{R,z}$ is above a threshold. The MBL phase is argued to have numerous localized (quasi)local conserved quantities, making the system (approximately) integrable.

(f) $(J_x, J_y, J_z) = (0.5, 0.5, 1), \mathbf{B} = (0, 0, 0), \mathbf{B}_R = (1, 0, 1)$. This is the XXZ model with independent random magnetic fields in the x and the z direction. In this case, we find the model is fully chaotic: the level spacing statistics shows the Wigner-Dyson statistics of the gaussian orthogonal ensemble (GOE), and the entanglement entropy of all the eigenstates show a perfect volume law (Fig. 8(f)). Accordingly, we find only $p_{A,0}$ and $p_{A,1}$ are obviously nonzero (main text Fig. 3(f)), which correspond well to the only two local subregion conserved quantities of the trivial identity matrix I_A and the subregion Hamiltonian H_A .

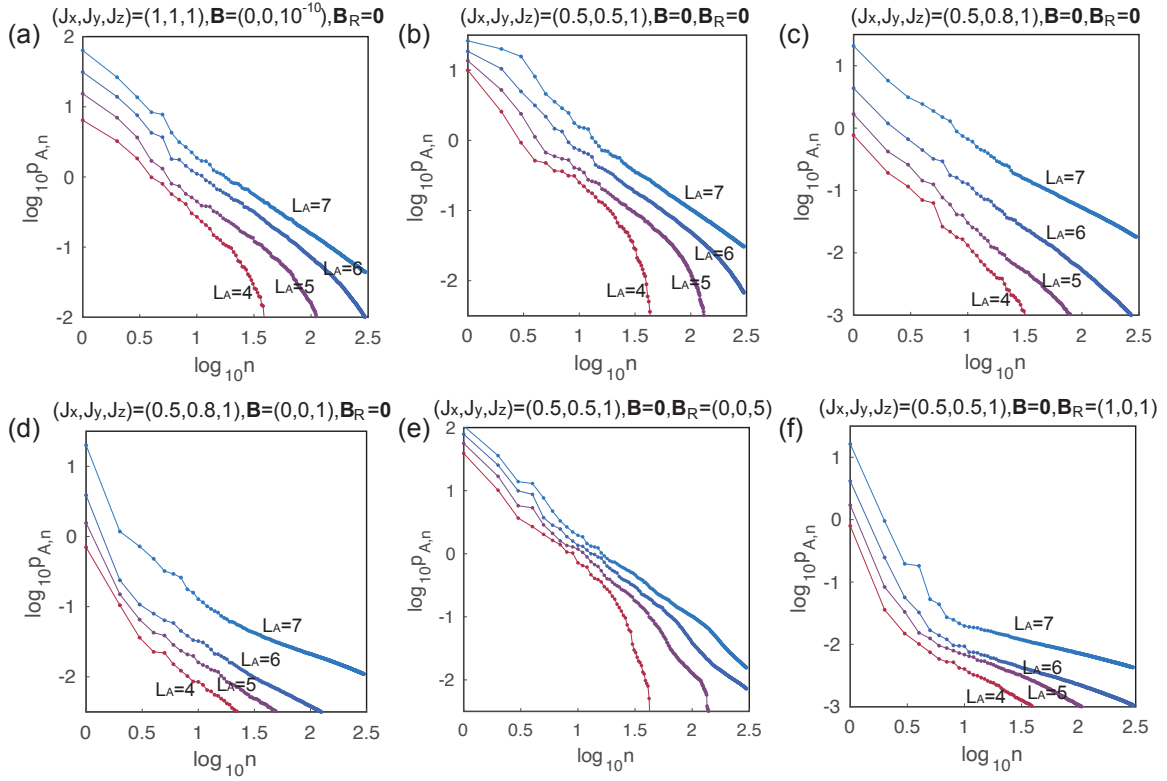


FIG. 7. The log-log plot of $\log_{10} p_{A,n}$ vs. $\log_{10} n$ for the EHS of the 1D XYZ model, calculated for an ensemble Ξ of all the eigenstates $|\alpha\rangle$ of the full system with equal weights w_α . The full system size is $L = 14$, and subregion A has size $L_A = 4, 5, 6, 7$. The parameters in each panel are the same as those in each panel of the main text Fig. 3, namely, this figure is the log-log plot of the main text Fig. 3. In panels (a)-(c) where the magnetic fields are zero, the XYZ model is translationally invariant and known to be integrable. Within the system size studied here, we find $p_{A,n}$ decays approximately as $p_{A,n} \propto n^{-s}$, where the exponent $s \approx 1$. In panel (e) where there is a random magnetic field in the z direction, the state is known to be in the MBL phase (see Fig. 8 for entanglement entropy evidence), which has localized quasilocal conserved quantities. Accordingly, we find $p_{A,n}$ also decays approximately in power law as $p_{A,n} \propto n^{-s}$, but the exponent $s \approx 1.5 \sim 2$ is larger than that in (a)-(c).

In the cases (a)-(d), as shown in Fig. 8(a)-(d), the majority eigenstates show a volume law entanglement entropy, and this is due to the existence of extended quasiparticle states in the system. In case (e) (Fig. 8(e)) where the system shows many-body localization, most eigenstates have small entanglement entropy due to the area law nature of the states. While in the fully chaotic case (f) (Fig. 8(f)), the eigenstates show perfect volume law entanglement entropies.

From the log-log plot of the EHS eigenvalues $p_{A,n}$ vs. n in Fig. 7, we find that within the limited system size we studied, $p_{A,n}$ of integrable systems approximately decay in a power law as $p_{A,n} \propto n^{-s}$. For parameters in Fig. 7(a)-(c) where the XYZ model is known to be analytically integrable, we find approximately $p_{A,n} \propto n^{-s}$, with the exponent $s \approx 1$. For Fig. 7(e) which is in the MBL phase, we also see $p_{A,n} \propto n^{-s}$ for a considerable range of n , with $s \approx 1.5 \sim 2$. More examples of MBL phase is shown in Fig. 9, where we see that the decaying exponent s has no obvious dependence on the parameters (generically around $s \approx 1.5 \sim 2.5$), as long as the system is in the MBL phase. When the random magnetic field increases (Fig. 9(b)), $p_{A,n}$ deviates more from the power-law decaying behavior, possibly because the system is closer to a non-interacting system (dominated by random fields).

Overall, for interacting integrable models, within the small system sizes we studied, we find power-law decay is a good fit for the EHS eigenvalues $p_{A,n}$. Enlarging the system size for interacting models is numerically difficult, and we leave the study of larger system sizes in the future.

In contrast, in Fig. 7 (f) which is fully chaotic, the decaying behavior of $p_{A,n}$ clearly deviates from a simple power-law decay. In the main text Fig. 3, one can see that only $p_{A,0}$ and $p_{A,1}$ are large, and we find their eigen-operators approximately give the identity I_A and subregion Hamiltonian H_A .

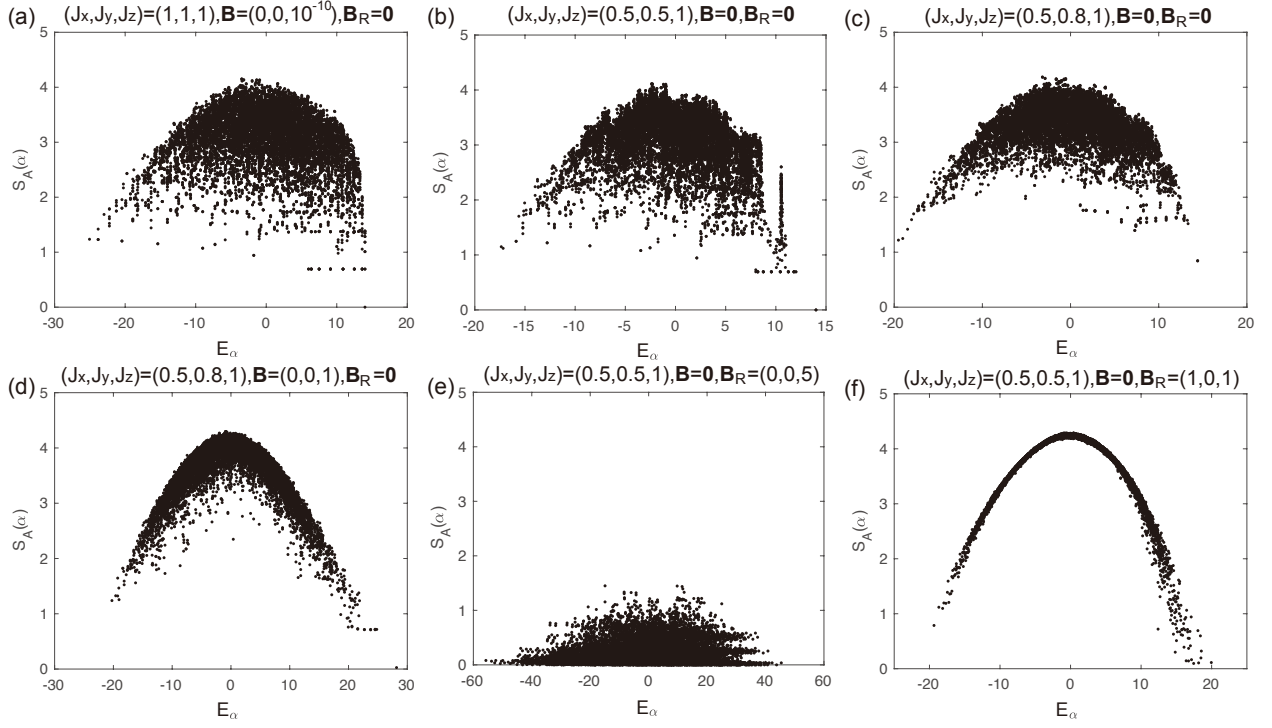


FIG. 8. The entanglement entropy of all the eigenstates, where the full system size $L = 14$, and subregion A has a size $L_A = 7$. The parameters in each panel is chosen the same as those in each panel of the main text Fig. 3.

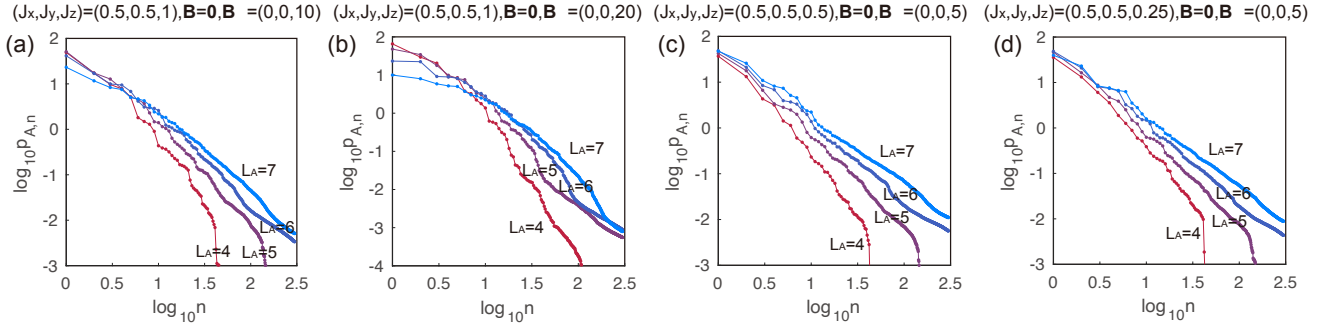


FIG. 9. More examples of log-log plot of the EHSM eigenvalues for systems in the MBL phase, where the full system size $L = 14$, and subregion A has a size $L_A = 7$. The parameters are labeled in each panel, which are all in the MBL phase.

B. How well the EHSM eigen-operators are conserved quantities

In this subsection, we test how well the EHSM eigenvectors (eigen-operators) $\overline{Q}_A^{(n)}$ (which are matrices in the Hilbert space) are conserved quantities in subregion A . To examine this, for each normalized eigen-operator $\overline{Q}_A^{(n)}$, we define a commutator-anticommutator ratio

$$r_A^{(n)} = \frac{\text{tr} \left(- \left[\overline{Q}_A^{(n)}, H_A \right]^2 \right)}{\text{tr} \left(\left\{ \overline{Q}_A^{(n)}, H_A \right\}^2 \right)}, \quad (67)$$

where H_A is the Hamiltonian in subregion A as defined in main text Eq. (2), while $[A, B] = AB - BA$ and $\{A, B\} = AB + BA$ stand for commutator and anticommutator, respectively. For Hermitian operators $\overline{Q}_A^{(n)}$, one has $r_A^{(n)} \geq 0$.

If $r_A^{(n)}$ is close to zero, $\bar{Q}_A^{(n)}$ will be a good conserved quantity of subregion A .

In Tab. S1 below, we list the commutator-anticommutator ratio of the first 7 EHSM eigen-operators $\bar{Q}_A^{(n)}$ ($0 \leq n \leq 6$) for the XYZ model with six groups of parameters given in the main text Fig. 3 (see also the supplementary Fig. 8), where the total system size $L = 14$ and subsystem size $L_A = 7$. As we can see, all the ratios $r_A^{(n)}$ are close to zero, indicating they are indeed approximate subregion A conserved quantities.

Fig. 3 label	XYZ model parameters	$r_A^{(0)}$	$r_A^{(1)}$	$r_A^{(2)}$	$r_A^{(3)}$	$r_A^{(4)}$	$r_A^{(5)}$	$r_A^{(6)}$
(a)	$(J_x, J_y, J_z) = (1, 1, 1), \mathbf{B} = (0, 0, 10^{-10}), \mathbf{B}_R = (0, 0, 0)$	0.0001	0.0014	0.0010	0.0067	0.0356	0.0443	0.1615
(b)	$(J_x, J_y, J_z) = (0.5, 0.5, 1), \mathbf{B} = (0, 0, 0), \mathbf{B}_R = (0, 0, 0)$	0.0001	0.0011	0.0011	0.0018	0.0476	0.0804	0.0240
(c)	$(J_x, J_y, J_z) = (0.5, 0.8, 1), \mathbf{B} = (0, 0, 0), \mathbf{B}_R = (0, 0, 0)$	0.0004	0.0012	0.0423	0.0356	0.0799	0.0188	0.0314
(d)	$(J_x, J_y, J_z) = (0.5, 0.8, 1), \mathbf{B} = (0, 0, 1), \mathbf{B}_R = (0, 0, 0)$	0.0001	0.0005	0.0010	0.0035	0.0025	0.0145	0.0143
(e)	$(J_x, J_y, J_z) = (0.5, 0.5, 1), \mathbf{B} = (0, 0, 0), \mathbf{B}_R = (0, 0, 5)$	0.0000	0.0001	0.0001	0.0002	0.0005	0.0004	0.0002
(f)	$(J_x, J_y, J_z) = (0.5, 0.5, 1), \mathbf{B} = (0, 0, 0), \mathbf{B}_R = (1, 0, 1)$	0.0002	0.0008	0.0048	0.0092	0.0294	0.0166	0.0190

TABLE S1. The commutator-anticommutator ratio $r_A^{(n)}$ for the leading 7 EHSM eigen-operators $\bar{Q}_A^{(n)}$ of the XYZ model, where the parameters are as labeled in the panels (a)-(f) of main text Fig. 3 (also supplementary Fig. 8), and the full system and subsystem sizes are $L = 14$ and $L_A = 7$.

C. Extracted subregion conserved quantities for the XXZ model

In this subsection, we discuss how the EHSM eigen-operators $\bar{Q}_A^{(n)}$ look like for the XXX model (main text Fig. 3(a)) and the XXZ model (main text Fig. 3(b)). Recall that the eigen-operators $\bar{Q}_A^{(n)}$ are sorted in the order of descending EHSM eigenvalues $p_{A,n}$ ($n \geq 0$).

Model parameter	XXX model (main text Fig. 3(a))					XXZ model (main text Fig. 3(b))				
Overlap ξ with	$\bar{Q}_A^{(0)}$	$\bar{Q}_A^{(1)}$	$\bar{Q}_A^{(2)}$	$\bar{Q}_A^{(3)}$	$\bar{Q}_A^{(4)}$	$\bar{Q}_A^{(0)}$	$\bar{Q}_A^{(1)}$	$\bar{Q}_A^{(2)}$	$\bar{Q}_A^{(3)}$	$\bar{Q}_A^{(4)}$
I_A	-0.995	0.010	-0.041	0.040	0.027	0.989	0.047	-0.035	-0.088	-0.011
H_A	0.043	-0.026	-0.963	0.061	0.091	-0.077	0.895	-0.283	-0.210	0.082
$\sum_i \sigma_{z,i}$	0.012	0.979	-0.023	0.024	-0.0156	0.059	0.355	0.768	0.463	0.098
$\sum_i \sigma_{x,i}$	0	0	0	-0.0002	-0.0003	0	0	0	0	0
$\sum_i \sigma_{z,i} \sigma_{z,i+1}$	0.020	-0.027	-0.551	0.151	-0.217	-0.079	0.725	-0.113	-0.350	0.244
$\sum_i \sigma_{x,i} \sigma_{x,i+1}$	0.027	-0.009	-0.558	-0.023	0.187	-0.015	0.372	-0.234	0.092	-0.144
$\sum_i \sigma_{y,i} \sigma_{y,i+1}$	0.027	-0.009	-0.558	-0.022	0.187	-0.015	0.372	-0.234	0.092	-0.144
$\sum_i \sigma_{z,i} \sigma_{z,i+2}$	0.011	-0.018	0.033	0.516	-0.152	-0.039	-0.006	0.324	-0.515	-0.007
$\sum_i \sigma_{x,i} \sigma_{x,i+2}$	0.019	-0.001	0.005	0.327	0.210	0.006	-0.012	0.022	-0.051	0.192
$\sum_i \sigma_{y,i} \sigma_{y,i+2}$	0.019	-0.001	0.005	0.327	0.210	0.006	-0.012	0.023	-0.050	0.192
$\sum_i \sigma_{z,i} \sigma_{z,i+3}$	0.021	-0.015	0.022	0.321	-0.263	-0.040	-0.024	0.251	-0.361	-0.265
$\sum_i \sigma_{x,i} \sigma_{x,i+3}$	0.027	-0.0003	-0.0007	0.170	0.058	-0.006	0.001	0.003	0.001	0.020
$\sum_i \sigma_{y,i} \sigma_{y,i+3}$	0.027	-0.0003	-0.0008	0.170	0.058	-0.006	0.001	0.003	0.001	0.020
$\sum_i \sigma_{z,i} \sigma_{z,i+4}$	0.008	-0.014	0.002	0.261	-0.236	-0.017	-0.018	0.174	-0.264	-0.203
$\sum_i \sigma_{x,i} \sigma_{x,i+4}$	0.013	-0.001	-0.015	0.143	0.005	0.003	0.003	0	-0.012	0.005
$\sum_i \sigma_{y,i} \sigma_{y,i+4}$	0.013	-0.001	-0.015	0.143	0.005	0.003	0.003	0	-0.012	0.005
$\sum_i \sigma_{z,i} \sigma_{z,i+1} \sigma_{z,i+2} \sigma_{z,i+3}$	-0.022	-0.001	-0.010	0.067	-0.099	0.039	0.035	-0.006	-0.112	0.009
$\sum_i \sigma_{z,i} \sigma_{x,i+1} \sigma_{x,i+2} \sigma_{z,i+3}$	-0.004	-0.0006	-0.033	-0.077	-0.230	-0.001	0.043	-0.038	0.032	-0.438
$\sum_i \sigma_{z,i} \sigma_{y,i+1} \sigma_{y,i+2} \sigma_{z,i+3}$	-0.004	-0.0006	-0.033	-0.077	-0.230	-0.001	0.043	-0.038	0.032	-0.438
$\sum_i \sigma_{x,i} \sigma_{z,i+1} \sigma_{z,i+2} \sigma_{x,i+3}$	-0.004	-0.0001	-0.044	-0.093	-0.215	0.002	0.017	-0.015	0.010	-0.080
$\sum_i \sigma_{y,i} \sigma_{z,i+1} \sigma_{z,i+2} \sigma_{y,i+3}$	-0.004	-0.0001	-0.044	-0.093	-0.215	0.002	0.017	-0.015	0.010	-0.080
$\sum_i \sigma_{x,i} \sigma_{y,i+1} \sigma_{y,i+2} \sigma_{x,i+3}$	-0.004	-0.0004	-0.047	-0.093	-0.215	0.001	0.031	-0.025	0.023	-0.172
$\sum_i \sigma_{y,i} \sigma_{x,i+1} \sigma_{x,i+2} \sigma_{y,i+3}$	-0.004	-0.0004	-0.047	-0.093	-0.215	0.001	0.031	-0.025	0.023	-0.172
P_3	0	0	0	0	0	0	0	0	0	0
P_4^{orth}	0.018	-0.007	-0.107	0.095	-0.506	-0.001	0.082	-0.075	0.066	-0.681

TABLE S2. The overlap of EHSM eigen-operators $\bar{Q}_A^{(n)}$ with various operators in subregion A , where the model parameters are given by the main text Fig. 3(a) (the zero field XXX model with $(J_x, J_y, J_z) = (1, 1, 1)$) and the main text Fig. 3(b) (the zero field XXZ model with $(J_x, J_y, J_z) = (0.5, 0.5, 1)$), respectively. The full system size is $L = 14$, and the subregion A size is $L_A = 7$.

In Tab. S2, we calculate the overlap between the numerical EHSM eigen-operators $\bar{Q}_A^{(n)}$ and various operators M_A in subregion A , which is defined as

$$\xi(\bar{Q}_A^{(n)}, M_A) = \frac{\text{tr}(\bar{Q}_A^{(n)} M_A)}{\|\bar{Q}_A^{(n)}\| \|M_A\|}. \quad (68)$$

Note that we have normalized $\|\bar{Q}_A^{(n)}\| = 1$. The parameters are as defined in the main text Fig. 3(a) (the XXX model) and in the main text Fig. 3(b) (the XXZ model), in both cases the magnetic field is zero.

In particular, we examine the overlaps of $\bar{Q}_A^{(n)}$ with the known analytical local conserved quantities P_n ($n = 3, 4$) [6, 7] generated by a boost operator K , as defined below. We first define the 3×3 matrix $J = \text{diag}(J_x, J_y, J_z)$. We can then rewrite the XYZ model without magnetic field Hamiltonian H and define the Boost operator K as

$$H = \sum_j \boldsymbol{\sigma}_j \cdot (J \boldsymbol{\sigma}_{j+1}), \quad K = \sum_j j \boldsymbol{\sigma}_j \cdot (J \boldsymbol{\sigma}_{j+1}). \quad (69)$$

Accordingly, a series of local conserved quantities are given by $P_3 = c_3[K, H]$, and $P_n = c_n[K, P_{n-1}]$, where c_n are only number factors which we choose for convenience. Note that P_n is generically n -supported, namely, all the terms in P_n are supported by no more than n neighboring sites. Here we only study the first two conserved quantities derived in this way, which are explicitly

$$P_3 = \frac{1}{2}[K, H] = \sum_j (J \boldsymbol{\sigma}_j) \cdot [\boldsymbol{\sigma}_{j+1} \times (J \boldsymbol{\sigma}_{j+2})], \quad (70)$$

and

$$P_4 = \frac{1}{4}[K, P_3] = \sum_{j,\nu} \left[\sum_{\mu} |\epsilon_{\mu\nu\lambda}| J_{\mu} J_{\lambda} \sigma_{j,\mu} \sigma_{\nu,j+1} (J_{\mu} \sigma_{\nu,j+2} \sigma_{\mu,j+3} - J_{\nu} \sigma_{\mu,j+2} \sigma_{\nu,j+3}) \right. \\ \left. + \sum_{\mu \neq \nu} J_{\mu}^2 J_{\nu} \sigma_{\nu,j} \sigma_{\nu,j+1} + J_x J_y J_z \sigma_{\nu,j-1} \sigma_{\nu,j+1} \right], \quad (71)$$

where $\epsilon_{\mu\nu\lambda}$ is the Levi-Civita symbol. We note that P_3 is orthogonal to H_A ($\text{tr}(P_3 H_A) = 0$), but P_4 is not orthogonal to the physical Hamiltonian H_A , namely, $\text{tr}(H_A P_4) \neq 0$. Therefore, we define a conserved quantity P_4^{orth} orthogonal to H_A as

$$P_4^{\text{orth}} = P_4 - \frac{\text{tr}(P_4 H_A)}{\|H_A\|^2} H_A. \quad (72)$$

Besides, we have $\text{tr}(P_3 P_4^{\text{orth}}) = 0$.

To a good approximation, we find generically $\bar{Q}_A^{(0)} \propto I_A$ in all the cases. For the XXZ models shown in Tab. S2, the first two nontrivial conserved quantities $\bar{Q}_A^{(1)}$ and $\bar{Q}_A^{(2)}$ are almost the linear combinations of the subregion Hamiltonian H_A and the total z -direction spin $\sum_i \sigma_{z,i}$. We find the 3rd conserved quantity to be approximately

$$\bar{Q}_A^{(3)} \approx \sum_j \sum_{\ell \geq 1} [\zeta_z(l) \sigma_{z,j} \sigma_{z,j+\ell} + \zeta_{\perp}(l) (\sigma_{x,j} \sigma_{x,j+\ell} + \sigma_{y,j} \sigma_{y,j+\ell})] + \zeta' \sum_j \sigma_{z,j}, \quad (73)$$

where $\zeta_z(l)$ and $\zeta_{\perp}(l)$ decay as l grows, and ζ' is some constant. For the example of the XXX model, $\zeta' \approx 0$. The 4th conserved quantity $\bar{Q}_A^{(4)}$ is dominated by 4-support operators. Accordingly, it has a major overlap with the 4-supported local conserved quantity P_4^{orth} in Eq. (72).

In particular, we note that none of the conserved quantities $\bar{Q}_A^{(n)}$ has a nonzero overlap with the local conserved quantity P_3 .